UNIVERSIDADE DE SÃO PAULO

ESCOLA DE ENGENHARIA DE SÃO CARLOS

DEPARTAMENTO DE HIDRÁULICA E SANEAMENTO

CÉSAR AMBROGI FERREIRA DO LAGO

IMPACTOS DAS MUDANÇAS CLIMÁTICAS SOBRE A DRENAGEM URBANA SUBTROPICAL COM TÉCNICAS COMPENSATORIAS

VERSÃO CORRIGIDA

SÃO CARLOS

2018

CÉSAR AMBROGI FERREIRA DO LAGO

IMPACTOS DAS MUDANÇAS CLIMÁTICAS SOBRE A DRENAGEM URBANA SUBTROPICAL COM TÉCNICAS COMPENSATORIAS

Dissertação apresentada à Escola de Engenharia de São Carlos, da Universidade de São Paulo, como parte dos requisitos para obtenção do título de Mestre em Ciências: Engenharia Hidráulica e Saneamento

Orientador: Prof. Dr. Eduardo Mario Mendiondo

VERSÃO CORRIGIDA

SÃO CARLOS

2018

Ficha catalográfica elaborada pela Biblioteca Prof. Dr. Sérgio Rodrigues Fontes da EESC/USP com os dados inseridos pelo(a) autor(a).

A172i

Ambrogi Ferreira do Lago, César
IMPACTOS DAS MUDANÇAS CLIMÁTICAS SOBRE A DRENAGEM URBANA SUBTROPICAL COM TÉCNICAS COMPENSATORIAS / César Ambrogi Ferreira do Lago; orientador Eduardo Mario Mendiondo. São Carlos, 2018.

Dissertação (Mestrado) - Programa de Pós-Graduação em Engenharia Hidráulica e Saneamento e Área de Concentração em Hidráulica e Saneamento -- Escola de Engenharia de São Carlos da Universidade de São Paulo, 2018.

1. Mudanças climáticas. 2. Drenagem urbana subtropical 3. Técnicas compensatórias. I. Título.

Eduardo Graziosi Silva - CRB - 8/8907

FOLHA DE JULGAMENTO

Candidato: Bacharel **CESAR AMBROGI FERREIRA DO LAGO.**

Título da dissertação: "Impactos das mudanças climáticas sobre a drenagem urbana subtropical com técnicas compensatórias".

Data da defesa: 21/03/2018.

Comissão Julgadora:	**Resultado:**
Prof. Dr. **Eduardo Mario Mendiondo** **(Orientador)** (Escola de Engenharia de São Carlos/EESC)	APROVADO
Prof. Dr. **Marco Aurélio Holanda de Castro** (Universidade Federal do Ceará/UFC)	Aprovado
Dr. **Marcio Hofheinz Giacomoni** (Universidade do Texas em San Antonio/UTSA)	Aprovado

Coordenador do Programa de Pós-Graduação em Engenharia Hidráulica e Saneamento:
Prof. Dr. **Eduardo Mario Mendiondo**

Presidente da Comissão de Pós-Graduação:
Prof. Associado **Luis Fernando Costa Alberto**

ACKNOWLEDGMENTS

I would like to thank Mario my supervisor, who guided and trusted me through my Master's program and helped me to organize my ideas.

I would also like to thank Altair Rosa and Marina de Macedo, my partners and friends who helped me with wisdom and patience.

I would also like to thank all my and friends at NIBH; it would have been harder without them.

A special thanks to Adenauer and Neuza, my parents, to my brother Conrado and my sister Sheila. Also, my best wishes to my nephew João di Lucca.

Thank you, Mariana Santana, for supporting me and listening to all my worries.

Thanks to all my friends in Campestre and Poços de Caldas, especially to Marquinho at this moment.

To all the members of Banda Lago for the funny and, sometimes, crazy moments.

To the PPGSHS secretaries, Sá and Priscila, for their attention and competence.

Finally, I would like to thank CAPES/PROEX for granting me a full scholarship and to the University of Sao Paulo for the infrastructure.

"*I hereby declare this written research is original, with no conflict of interest, and complies with Codes of Ethics of the main research funding agencies and higher education boards, either Brazilian or International ones*".

Resumo

DO LAGO, C. A. F. (2018) **Impactos das mudanças climáticas sobre a drenagem urbana subtropical com técnicas compensatórias**. Dissertação, Escola de Engenharia de São Carlos, Universidade de São Paulo.

Técnicas compensatórias de drenagem (TC) vêm sido utilizadas para mitigar efeitos da urbanização no ciclo hidrológico. Entretanto faltam estudos sobre a performance destas TCs em clima subtropical e sob potenciais impactos de cenários de mudanças climáticas. Esta dissertação avaliou os impactos de dois cenários de mudanças climáticas (RCP 4.5 e 8.5) sobre o escoamento superficial urbano com poluentes e sua afetação na eficiência da TC localizada em clima subtropical, classificação Cfa segundo Köppen e Geiger. Primeiro se calibrou os parâmetros de quantidade e qualidade do escoamento superficial na entrada da biorretenção. O modelo buildup/washoff foi avaliado, comparando-se calibração da carga e concentração de poluentes: demanda química de oxigênio (DQO), carbono orgânico total (TOC), fosfato (PO4), nitrato (NO3), nitrito (NO2) amônia (NH3), ferro (Fe), cadmio (Cd) e zinco (Zn). Então se estudou a lavagem de poluentes na área de contribuição da biorretenção com histórico de precipitação entre 2013 e 2017 e analisando a influência dos parâmetros buildup/washoff de cada poluente na entrada de massa. Em seguida, cenários de mudanças climáticas Eta-5x5km (INPE) foram desagregados em intervalos de 5 minutos, pelo método de Bartlett-Lewis modificado. A série desagregada foi utilizada para se estimar os impactos das mudanças climáticas na drenagem urbana, a incidir na biorretenção. Então um modelo simples desenvolvido especificamente para a biorretenção em estudo foi usado para se estimar as eficiências quali-quantitativas de cada período dos cenários de mudanças climáticas. Os dados adquiridos do Inpe mostram que as mudanças climáticas resultarão em uma queda no volume de chuvas em São Carlos, resultando em menores volumes de escoamento superficial. Os impactos na lavagem de poluentes, entretanto, variam de acordo com os parâmetros buildup/washoff, explicados por uma análise de sensibilidade. As mudanças climáticas pouco afetam a eficiência quantitativa da biorretenção, 81.7% no período 1980-1999 para 81.4% e 81.3% no período 2080-2099 para cenários RCP 4.5 e 8.5. Já as eficiências de remoção de poluentes, assim como a lavagem destes, dependem das características buildup/washoff de lavagem. Uma das principais consequências observadas das mudanças climáticas é uma queda na qualidade do escoamento. Porém, mesmo com eficiência quantitativa sendo mantida, a biorretenção é capaz de amenizar essa o aumento na concentração de poluentes na drenagem urbana. Assim, a técnica ajudará a preservar a qualidade dos rios à jusante, que já terão seus volumes diminuídos pela queda no volume de chuva.

Palavras chave: Mudanças climáticas, drenagem urbana subtropical, técnicas compensatórias.

Abstract

DO LAGO, C. A. F. (2018) **Climate Changes Impacts on Subtropical Urban Drainage with Low Impact Developments**. Dissertation, São Carlos School of Engineering, University of São Paulo.

Low impact developments (LID) have been used to mitigate the effects of urbanization on the hydrological cycle. However, there is a lack of studies on LID performance in subtropical climates and under potential impacts of climate change scenarios. This dissertation evaluated the impacts of two climate change scenarios (RCP 4.5 and 8.5) on urban drainage with pollutants and their effect on LID practice efficiency located in a subtropical climate, with Cfa classification according to Köppen and Geiger. First, the inlet quantity and quality parameters were calibrated. The buildup/washoff model was evaluated, comparing load calibration and concentration of pollutants: chemical oxygen demand (COD), total organic carbon (TOC), phosphate (PO4) (NH3), iron (Fe), cadmium (Cd) and zinc (Zn). Pollutant washing was studied in the area of the bioretention catchment using historical rainfall data between 2013 and 2017, analyzing the influence of the buildup/washoff parameters of each pollutant in the input mass. Afterwards, Eta-5x5km (INPE) climate change scenarios were disaggregated to 5-minute intervals by the modified Bartlett-Lewis method. The disaggregated series was used to estimate the impacts of climate change on urban drainage into the bioretention. Therefore, a simple model, developed specifically for the study bioretention cell, was used to estimate the qualitative-quantitative efficiencies of each period of the climate change scenarios. According to the data acquired from INPE, climate change will result in a fall in the volume of rainfall in São Carlos, resulting in lower volumes of surface runoff. The impacts on pollutant washing, however, vary according to the buildup/washoff parameters, explained by a sensitivity analysis. Climate change does not affect the bioretention quantitative efficiency very much: 81.7% from 1980 to 1999 to 81.4% and 81.3% from 2080 to 2099 for CPR scenarios 4.5 and 8.5. The pollutant removal efficiencies, as well as the washing, depend on buildup/washoff characteristics. One of the main consequences of climate change is a drop in the runoff quality. However, even with quantitative efficiency being maintained, bioretention is capable of mitigating this increase in the concentration of pollutants in urban drainage. Thus, the LID will help preserve the quality of downstream rivers, whose volumes will already have diminished by the decrease in rainfall volume.

Key words: Climate changes, subtropical urban drainage, low impact developments.

Table of contents

1. INTRODUCTION 1

1.1.Research hypothesis 2

1.2. Purposes 2

1.3. Text organization 2

1.4. References 3

2.GENERAL METHODOLOGY 5

3.RUNOFF QUALITY AND QUANTITY PREDICTIONS IN A SUBTROPICAL CATCHMENT USING A BUILDUP/WASHOFF MODEL 8

3.1. Introduction 10

3.2. Methodology 11

3.2.1. Study Area 12

3.2.2. Data collection 13

3.2.3. Quantity calibration and simulation 14

3.2.4. Quality calibration and simulation 15

3.2.5. Quality sensitivity analysis 18

3.3. Results and discussion 19

3.3.1. Quantity calibration and validation 19

3.3.2. Sensitivity analysis of the model warm up 22

3.3.3. Washoff and buildup sensitivity analysis 23

3.3.4. Quality calibration and validation 28

3.3.5. Runoff characterization 31

3.4. Conclusions 35

3.5. References 36

4. EFFECTS OF CLIMATE CHANGE ON LOW IMPACT DEVELOPMENT (LID) PERFORMANCE - A CASE OF STUDY IN SAO CARLOS, BRAZIL 41

4.1.Introduction 42

4.2.Methodology 43

4.2.1.Study area and data collection 43

4.2.2.Bioretention outflow model 44

4.2.3.Climate Change Scenarios 47
4.3.Results 49
4.3.1. Outflow calibration and validation 49
4.3.2. Bioretention performance 50
4.3.3.Rainfall desegregation and climate changes in Sao Carlos 55
4.3.4.Climate change impacts on bioretention performance 57
4.4.Conclusions 61
4.5. References 62

5.GENERAL CONCLUSIONS 66

APPENDIX 69

1. INTRODUCTION

Most of the world population is currently living in urban areas. In Brazil, approximately 185 million people live in cities. This way of life alters the natural environment and one of the impacts is on the hydrologic cycle. Urbanization results in higher imperviousness, increasing runoff volume and its peak flows (Guan, Sillanpää, & Koivusalo, 2015), resulting in more frequent floods (Sun, Tong & Yang 2016, Sun et al. 2017) with a higher amount of pollutants washed-off (Fletcher, Andrieu & Hamel, 2013), degrading the quality of water bodies. Low Impact Developments (LID) practices have been used to prevent and mitigate such impacts, by treating the quantity and the quality of the stormwater.

However, LID in subtropical climates need to be better studied to verify their singularities and what their impacts are on the performance of LID (Macedo et al., 2017) as different rainfall regimes change the runoff generation and pollutant washoff processes. In the tropics, for example, higher intensity rainfall generates runoff more quickly (Le et al., 2007), resulting in major impacts on its quality (Piro & Carbone, 2014) and possibly on pollutants removal efficiency in LID practices. Therefore, the quantity and quality of runoff in tropical regions also needs to be better evaluated to carry out LID studies in these areas.

Rainfall regimes differ not only spatially, but also temporally as climate change models suggest. These changes tend to decrease the rainfall volume and increase its intensity, worsening water insecurity in the country due to more frequent occurrences of floods and droughts (Chou et al., 2014-a; Chou et al., 2014-b; Lyra et al., 2017; Marengo & Ambrizzi, 2014). LID practices are an alternative to mitigate these climate change impacts, which will possibly also alter LID practice performances.

This research studied the quality of stormwater in a subtropical catchment in São Carlos, relating the pollutant washoff process to some rainfall event characteristics such as intensity and previous dry days. Then, climate changes scenarios were evaluated and their impacts on bioretention cell quality and quantity efficiencies were analyzed and discussed.

1.1.Research hypothesis

The effects of a progressive augmentation of rainfall extremes, caused by climate changes, influences the rainfall-runoff process in subtropical urban areas, decreasing stormwater retention and pollutant removal performance of LID practices.

1.2. Purposes

1.3.1. General purpose

To elucidate how runoff generation and pollutant wash-off processes respond to upstream factors of an experimental LID technique and evaluate how this practice would perform as a local adaptation strategy considering rainfall-runoff scenarios under climate change.

3.1.2. Specific purposes

1. Characterize the urban runoff in a subtropical catchment, in terms of volume, flow and water quality, elucidating the runoff generation and pollutant wash-off processing, using a stepwise flowchart including calibration, validation and sensitivity analysis.

2. Analyze the impacts of climate changes on subtropical urban drainage.

1.3. Text organization

Chapter 2 describes the general methodology. It briefly explains how chapters are connected and how they contribute to the general and specific purposes.

In **Chapter 3**, the runoff generation and pollutant washoff processes in a subtropical climate drained to the bioretention are discussed. This was important for better precision in the quality predictions as two calibration methods were compared in this chapter (concentration and load-based calibration).

Chapter 4 analyzes the bioretention performance and verifies the climate changes in São Carlos for the RCP 4.5 and 8.5 scenarios. Future periods (2020-2039, 2040-2059, 2060-2079, and 2080-2099) were compared to the present date (1980-1999), and therefore the changes occurring in one century could be estimated.

Finally, **Chapter 5** includes the general conclusions and recommendations for future research to better understand this dissertation.

1.4. References

Chou, S. C., Lyra, A., Mourão, C., Dereczynski, C., Pilotto, I., Gomes, J., ... & Campos, D. (2014). Evaluation of the Eta simulations nested in three global climate models. *American Journal of Climate Change*, *3*(5), 438-454.

Chou, S. C., Lyra, A., Mourão, C., Dereczynski, C., Pilotto, I., Gomes, J., ... & Campos, D. (2014). Assessment of climate change over South America under RCP 4.5 and 8.5 downscaling scenarios. *American Journal of Climate Change*, *3*(5), 512-525.

Fletcher, T. D.; Andrieu, H.; Hamel, P. Understanding, management and modelling of urban hydrology and its consequences for receiving waters: A state of the art. *Advances in Water Resources*, v. 51, p. 261-279, 2013.

Guan, M., Sillanpää, N., & Koivusalo, H. (2015). Modelling and assessment of hydrological changes in a developing urban catchment. *Hydrological Processes*, *29*(13), 2880-2894.

Le, S. H., Chua, L. H. C., Irvine, K. N., & Eikaas, H. S. (2017). Modeling washoff of total suspended solids in the tropics. *Journal of Environmental Management*, *200*, 263-274.

Macedo, M. B., Rosa, A., do Lago, C. A. F., Mendiondo, E. M., & de Souza, V. C. B. (2017). Learning from the operation, pathology and maintenance of a bioretention system to optimize urban drainage practices. *Journal of Environmental Management*, *204*, 454-466.

Lyra, A., Tavares, P., Chou, S. C., Sueiro, G., Dereczynski, C., Sondermann, M., ... & Giarolla, A. (2016). Climate change projections over three metropolitan regions in Southeast Brazil using the non-hydrostatic Eta regional climate model at 5-km resolution. *Theoretical and Applied Climatology*, 1-20.

Marengo, J. & Ambrizzi, T. (2014) Instituto Nacional de Ciência e Tecnologia de Mudanças Climáticas II. *Processo CNPq 465501/2014-1*, INCT-MC-II (FAPESP 2014/50848-9).

Sun, S., Barraud, S., Branger, F., Braud, I., & Castebrunet, H. (2017). Urban hydrologic trend analysis based on rainfall and runoff data analysis and conceptual model calibration. *Hydrological Processes*, *31*(6), 1349-1359.

Sun, Y., Tong, S., & Yang, Y. J. (2016). Modeling the cost-effectiveness of stormwater best management practices in an urban watershed in Las Vegas Valley. *Applied Geography*, *76*, 49-61.

Piro, P., & Carbone, M. (2014). A modelling approach to assessing variations of total suspended solids (TSS) mass fluxes during storm events. *Hydrological Processes*, *28*(4), 2419-2426.

2.GENERAL METHODOLOGY

The study area has 2.3ha, which presents 22% of impervious area. There is a 60m^2 bioretention downstream, where several events were monitored and used to calibrate and validate the inlet and outlet quantity and quality of the stormwater. Figure 2.1 illustrates the catchment and bioretention location.

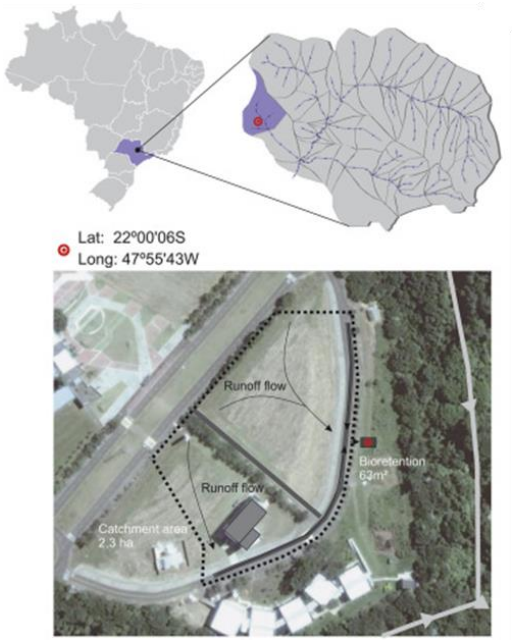

Figure 2.1: The bioretention location and its catchment.
Source: Adapted from Macedo (2017).

In Chapter 3, a sensitivity analysis of the buildup/washoff parameters of the pollutants was performed to understand their influence on the concentrations of the simulated runoff pollutants and better understand this process in the subtropical catchment and minimum warm-up period for reliable quality predictions. Two quality calibration methods were also compared in this chapter, a load-based and a concentration-based calibration to verify which correspond better to the purpose of this study. The quality simulations were done with observed discharge and were optimized using the GRG nonlinear solver tool, and was therefore performed on a spreadsheet.

Chapter 4 aims to evaluate the impacts of climate change on the rainfall regime, runoff and on the bioretention performance. The RCP scenarios 4.5 and 8.5 were used with downscaling based on the Eta Regional Climate Model forced by the global HadGEM2-ES model (Chou et al., 2014-a; Chou et al, 2014-b; Lyra et al, 2017). The data were acquired with a spatial scale of 5km and a 3-hour time scale, which was later reduced to 5min through a modified Bartlett-Lewis rectangular pulse model to simulate the runoff and pollutants into the bioretention. Regarding its outflow, a specific model was used for a greater accuracy of the ponding depth in the surface of the bioretention, which has a triangular weir for the outflow.

Figure 2.2. shows the general methodology flowchart, how chapter 3 and 4 are related and how they contribute to the general and specific purposes.

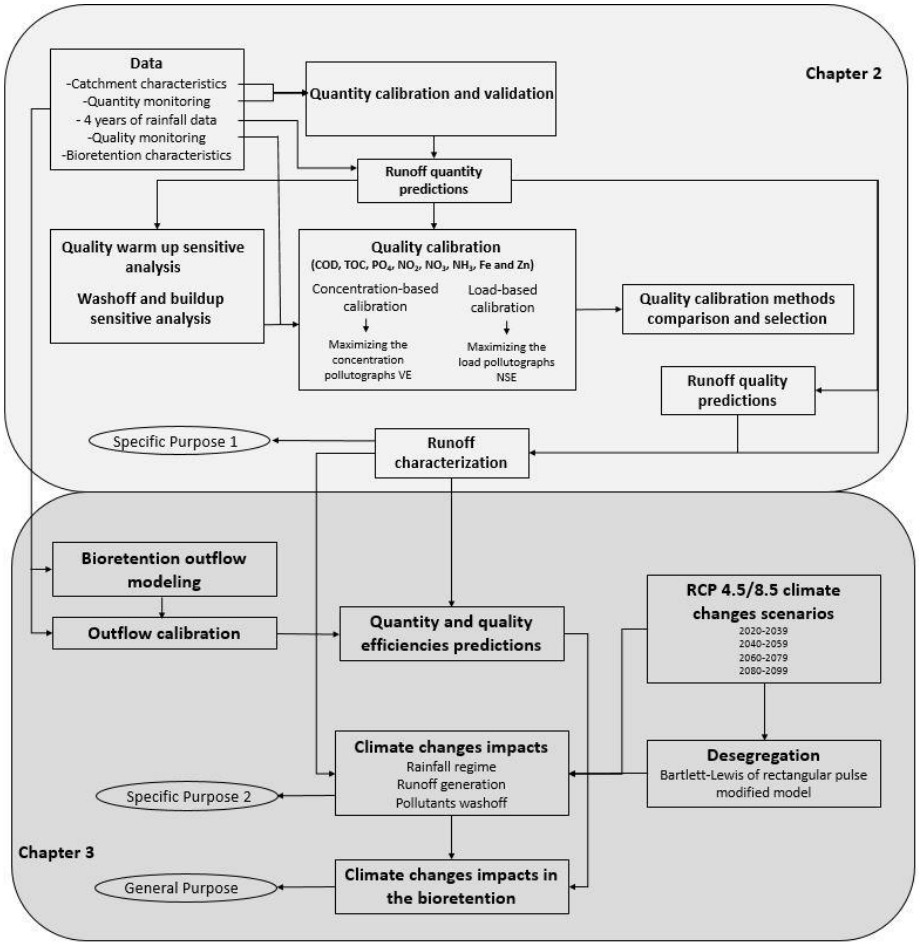

Figure 2.2. General methodology flowchart.

References

Chou, S. C., Lyra, A., Mourão, C., Dereczynski, C., Pilotto, I., Gomes, J., ... & Campos, D. (2014). Evaluation of the Eta simulations nested in three global climate models. *American Journal of Climate Change*, *3*(5), 438-454.

Chou, S. C., Lyra, A., Mourão, C., Dereczynski, C., Pilotto, I., Gomes, J., ... & Campos, D. (2014). Assessment of climate change over South America under RCP 4.5 and 8.5 downscaling scenarios. *American Journal of Climate Change*, *3*(5), 512-525.

Macedo, M. B., Rosa, A., do Lago, C. A. F., Mendiondo, E. M., & de Souza, V. C. B. (2017). Learning from the operation, pathology and maintenance of a bioretention system to optimize urban drainage practices. *Journal of Environmental Management*, *204*, 454-466.

Lyra, A., Tavares, P., Chou, S. C., Sueiro, G., Dereczynski, C., Sondermann, M., ... & Giarolla, A. (2016). Climate change projections over three metropolitan regions in Southeast Brazil using the non-hydrostatic Eta regional climate model at 5-km resolution. *Theoretical and Applied Climatology*, 1-20.

3.RUNOFF QUALITY AND QUANTITY PREDICTIONS IN A SUBTROPICAL CATCHMENT USING A BUILDUP/WASHOFF MODEL

A modified version of this chapter will be submitted as: César Ambrogi Ferreira do LAGO et al., Runoff quality and quantity predictions in a subtropical catchment using a buildup/washoff model.

Abstract

Hydrological modeling is an important tool for assessing catchment management plans. However, runoff quality modeling in urban catchments requires a better understanding, especially in tropical regions where high intensity rainfalls result in faster hydrological response. The aim of this paper is to qualitatively and quantitatively characterize the urban runoff in a subtropical catchment using a stepwise flowchart including calibration, validation, sensitivity analysis, as well as historical records. The calibration and validation of the runoff quantity were first performed considering six monitored events. Afterwards, different warm up periods of the quality model were analyzed concerning their influence on the initial buildup. In addition, a sensitivity analysis of the buildup and washoff parameters was carried out for a tropical rainfall regime. Then, two types of quality calibrations were evaluated: (1) the maximization of the Volumetric Efficiency (VE) of concentration; and (2) the maximization of the Nash-Sutcliffe Efficiency (NSE) of the pollutant load. Both methods were carried out using observed discharge to avoid propagation of quantitative simulation errors. After validating the quality model, four years of rainfall data were used to simulate and characterize the runoff. Our findings showed that warming up the quality model played an important role in the initial buildup, which could be under-estimated in 93% in one of the events if only considering the previous dry days. Calibrating the concentrations, as expected, generates smaller differences in the predicted and observed mean concentrations. However, by maximizing the NSE of the load pollutograph, the total pollutant mass (and consequently the Event Mean Concentration (EMC)) were more compatible, and were

therefore used for the simulations. Over 4 years, it is estimated that approximately 1223 mm (or 29,000m^3) of runoff washed approximately 9659g/ha, 3818.2g/ha, 93.8g/ha, 306.9g/ha, 29731g/ha, 475.5g/ha of Fe, NO_3, NO_2, PO_4, TOC and Zn, respectively. Most of the pollutant mass was generated in the summer (rainy season), while the highest EMCs were found during the winter (dry season). A nonlinear relationship was also observed between the total runoff volume and pollutant mass for higher values of washoff coefficient ($w1$).

Key-words: Subtropical quality modeling, buildup/washoff, sensitivity analysis

3.1. Introduction

Urbanization accelerates hydrologic responses increasing runoff volume and peak flows (Guan, Sillanpää, & Koivusalo, 2015), leading to more flood risks (Sun, Tong & Yang 2016, Sun et al. 2017) and the amount of transported pollutants (Flecther, Andrieu & Hamel, 2013). Monitoring urban catchments requires time, funding and depends on random variables, such as rainfall intensity, making it difficult to understand the system more comprehensively.

Using watershed models to predict runoff discharges can be used as a tool to better evaluate BMPs and watershed management plans (Borah, 2011). Predicting water quality can also be used to support decision makers. Rode et al. (2005) stated that runoff quality models are essential for watershed management plans. However, quality modeling as a management tool is still incipient in Brazilian catchments. For instance, there are considerable uncertainties in studies addressing pollutant load generation under land-use change (Zaffani et al, 2015), quali-quantitative field experiments (Taffarello et al, 2016) and modeling scenarios of nested catchments (Taffarello, 2017).

The phenomenon involved in stormwater quality needs to be better understood for more reliable quality simulations (Obropta & Kardos , 2007; Bonhomme & Petrucci, 2017), especially in the tropics where high intensity rainfall generates faster runoff responses (Le et al., 2007). In wet climates, the interaction between the catchment hydrology and the accumulation and transportation of pollutants has a major impact on the quality of the runoff (Piro & Carbone, 2014).

Liu et al. (2014) and Rosa (2016) analyzed hydrologic models with qualitative aspects, possibly using BMP. In this paper, eight models were analyzed, including the Storm Water Management Model (SWMM), the Hydrologic Modeling System (HEC-HMS), DRAINMOD

and RECARGA in the public domain. They also show that only the SWMM and the RECARGA incorporate qualitative modeling, and the SWMM is most used worldwide.

SWMM uses the buildup/washoff model. It consists of the runoff washing the pollutants, which were deposited during the dry period. The model needs calibration and even doing so, the uncertainties remain (Bertrand-Krajewski, 2007).

This study analyzed the quality of stormwater in a subtropical catchment, classified as Cfa as Köppen e Geiger,. A sensitivity analysis of the buildup/washoff parameters was performed to understand their influence on the concentrations of the simulated runoff pollutants. Two quality calibration methods were also analyzed: a load-based and a concentration-based calibration. The article includes a comprehensive flowchart of the methodology (Section 2), with calibration and validation steps (Sections 2.3 and 2.4), a sensitivity analysis related to the model warm-up (Section 2.5) and results and discussions using a subtropical rainfall regime (Section 3).

3.2. Methodology

The methodology that characterizes the runoff is summarized in a flowchart in Figure 3.1. See further details in the text.

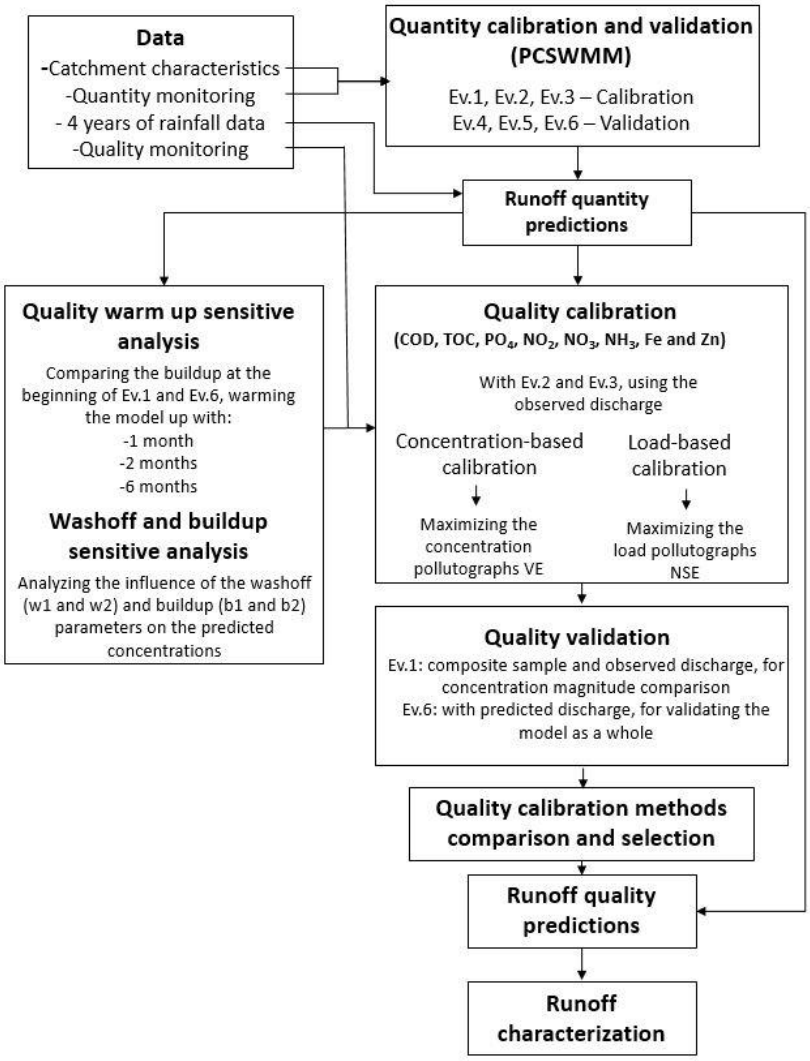

Figure 3.1: Methodology flowchart used in this chapter.

3.2.1. Study Area

The studied catchment is located at Campus 2 at the University of São Paulo (USP), São Carlos, Brazil. The city has a subtropical climate with an average annual rainfall of 1422mm. January (summer) is the month that has a higher precipitation volume with an average of 269mm, while July (winter) has the lowest with an average of 15.5mm (Miranda et al., 2012).

The area has 2.3 hectares, which presents 22% of impervious area related to buildings, roads and footpaths, while the pervious part is mainly covered by short grass. The local soil was analyzed, resulting in 20% clay, 10% silt and 70% sand, and was classified between sandy clay loam and sandy loam soils *(USDA, 2017).* The average slope of the area is 3.5%, which was obtained using the Digital Elevation Model (DEM). Downstream of the area is a 60.6m³ bioretention, where the data were collected (Macedo et al., 2017).

The campus is under an occupation process and the impervious area is expected to reach 50% by 2025 and 80% by 2100 (Rosa, 2016). However, no building was under construction during the data collection, which would have had a strong impact on the generation of pollutants (Sillanpää & Koivusalo, 2015).

3.2.2. Data collection

Data from seven monitored events were used for the quali-quantity calibration and their characteristics are shown in Table 3.1. A rain gauge with a 0.2mm precision was used to obtain the rainfall data, installed at the campus about 400m from the catchment. Quality data in Ev.1 was collected as composite sample and Ev. 6 has no quantity data.

Table 3.1: Monitored events and their characteristics.

	Day	Prior dry period (days)	Observed runoff duration (min)	Total precipitation (mm)	Average precipitation intensity (mm/hr)	Monitoring Type
Ev.1	25/08/2015	29	89	3.8	3.3	Quantity and quality*
Ev.2	27/08/2015	0	137	1.8	1.7	Quantity and quality
Ev.3	08/09/2015	1	478	37.8	5.1	Quantity and quality
Ev.4	02/09/2016	1	118	6.4	11.6	Quantity
Ev.5	06/09/2016	3	211	7.0	2.8	Quantity
Ev.6	16/05/2016	0	**53	5.8	20.5	Quality
Ev.7	26/04/2017	0	632	18.4	2	Quantity

Note: *Composite sample ** Predicted runoff duration

The quantity data was obtained by a water level sensor (HOBO Water Level U20l-02) placed in a composed weir, both triangular and rectangular, located at the bioretention entrance.

The water level, which was registered every minute, was then converted to discharge with calibrated weir.

Concerning the quality, Event (Ev)1 presents a composite sample acquired during the first 30 minutes. Samples from Ev.2 and Ev.3 were collected every 4 minutes in the first 24 minutes of the events. In Ev.6, they were collected every 5 minutes during the first 50 minutes. The concentrations of chemical oxygen demand (COD), total organic carbon (TOC), phosphate (PO_4), nitrate (NO_3), nitrite (NO_2) ammonia (NH_3), iron (Fe), cadmium (Cd) and zinc (Zn) were obtained from the laboratory using the Standard Methods for the Examination of Water and Wastewater (APHA et al., 2005).

3.2.3. Quantity calibration and simulation

The PCSWMM software was used to simulate the runoff quantity. Its calibration was performed with Ev.1, Ev.2 and Ev.3 with total rainfall ranging from 1.8mm to 37.8mm, and the intensity from 1.7mm / hr to 5.1mm / hr. It was validated using Ev.4, Ev.5 and Ev.7 with a variation between 6.4 mm and 18.4 mm total rainfall, with an intensity varying between 2 mm / hr and 11.5 mm / hr. Thus, the calibration was done covering a wider range of total precipitated volume, while for validation, a greater variation of rainfall intensity. Both the calibration and validation were carried out using a 1 min timestep.

The calibration was continuous, which was manually performed using the rainfall data from 25/08/2015 to 08/09/2015 including Ev.1, 2 and 3. The validation was also continuous from Ev.4 to Ev.5, but singular for Ev.7. The effectiveness of the calibration and validation was evaluated individually for each event using the Nash-Sutcliffe Efficiency (NSE), R^2, total runoff volume and the maximum peak difference.

After the calibration and validation were completed, (03/20/2013 to 03/20/2017) rainfall data collected over 4 years were used to simulate the runoff quality and quantity in PCSWMM. The date of 20th March was chosen because it is when the autumn season starts in the southern hemisphere. Thus, 16 seasons were included in this period and Table 3.2 shows their characteristics. As it covers a long period, a 5 min timestep for the simulation was used, rather than 1 minute for quality and quantity calibration and validation. In São Carlos, there are only two well defined seasons, which are summer and winter. Autumn and spring were analyzed as post wet and dry seasons, respectively.

Table 3.2: Rainfall characteristics in each considered season

	Rainfall (mm)			
Seasons	**Year 1 (2013-2014)**	**Year 2 (2014-2015)**	**Year 3 (2015-2016)**	**Year 4 (2016-2017)**
Autumn (March 20th to June 21st)	194.4	107.0	182.0	277.8
Winter (June 21st to September 22nd)	92.2	88.8	168.6	5.2
Spring (September 22nd to December 21st)	329.4	364.6	200.4	543.6
Summer (December 21st to March 20th)	345.4	592.6	527.4	624.8
Year Total	961.4	1153.0	1078.4	1451.4

3.2.4. Quality calibration and simulation

Quantity simulations were done using buildup/washoff model, which is described below. Its calibration was performed using Ev.2 and Ev.3, while the validation was carried out using Ev.1 and Ev.6. The predicted discharge obtained from the quantity simulation was used for a continuous calibration and validation with 6 months of warm-up. To avoid propagating errors from the quantity prediction to the quality calibration, the observed discharge was used for Ev.2 and Ev.3. Validation was carried out using the predicted discharge and Ev.1 was used only to compare the simulated mean concentrations with the one found in the composite sample, and also to verify if their magnitudes corresponded.

The quality calibration was performed according to two methodologies: one calibrating the pollutant load and the other calibrating their concentration. The load-based calibration aimed to maximize the NSE of the load pollutograph, given by Equation (1) (Nash, & Sutcliffe, 1970), while the concentration-based calibration was done by maximizing the Volumetric Efficiency (VE) of the concentration, proposed by Criss & Winston (2008) and shown in Equation (2). VE was used, rather than the sum of the square difference, for an equal weight in the events as the simple sum of the square difference would generate larger results for the events with larger concentrations. This equation was also preferred to the difference between the means of the simulated and observed concentrations, because this can mark a difference between instantaneous concentrations in different periods. Furthermore, the NSE was not used for concentration-based calibration as some concentrations tended to be constant and steady observed values may result in large negative values, not necessarily representing a very poor result (Criss & Winston, 2008). The buildup and washoff parameters were adjusted until the observed and simulated values were closed, then the EXCEL solver tool (non-linear GRG) was used to refine their values.

The difference of the mean concentrations and of total income mass, VE, NSE and R^2 were used to evaluate the quality model. Concentration outliers were identified and not considered during the model evaluation.

$$NSE = 1 - \frac{\sum\left(C_{obs(t)} - C_{sim(t)}\right)^2}{\sum\left(C_{obs(t)} - \overline{C_{obs}}\right)^2} \quad (1)$$

$$VE_{(x)} = 1 - \frac{\sum\left|C_{sim(t)} - C_{obs(t)}\right|}{\sum C_{obs(t)}} \quad (2)$$

where, $NSE_{(x)}$ is the Nash-Sutcliffe efficiency for pollutant x, $C_{obs(t)}$ is the *t*-th observed concentration, $C_{sim(t)}$ is the simulated concentration in *t*-th and $\overline{C_{obs}}$ is the average of observed concentrations.

To simulate the runoff quality, the same exponential buildup and washoff equations used in SWMM (Rossman, 2010) were chosen and adapted for this study. Equation (3) describes the washoff exponential equation.

$$W_{(t)} = \frac{w1.q^{w2}.B_{(t)}.A}{60} \tag{3}$$

where $W_{(t)}$ is the *t*-th washoff [kg/min], *w*1 is the washoff coefficient, *w*2 is the washoff exponent, q is the runoff rate [mm/h], $B_{(t)}$ is the buildup in the *t*-th time [kg/ha] and A is the catchment area [ha].

However, if the result of Equation (3) is higher than the disposal buildup, the washoff would be given by Equation (4):

$$W_t = B_{(t)}.A \tag{4}$$

The buildup equation depends if the washoff has occurred or not, as follows:

$$B_{(t)} = \begin{cases} B_{(t-1)} - \dfrac{W_{(t-1)}}{A} & if\ W_{(t-1)} > 0 \\ b1\left(1 - e^{-\frac{b2}{1440}T_{(t)}}\right) & if\ W_{(t-1)} = 0 \end{cases} \tag{5}$$

where *b*1 is the maximum buildup [kg/ha], *b*2 is buildup exponent [1/days] and $T_{(t)}$ is the previous dry period [min]. Each buildup/washoff parameters physical meaning are better described in the sensitivity analysis (section 3.3.2).

The previous dry period also considers the washoff. If the washoff occurred, time $T_{(t)}$ will be the number of previous dry days corresponding to the remaining buildup.

$$T_{(t)} = \begin{cases} \dfrac{ln\left(1 - \dfrac{B_{(t)}}{b1}\right)}{b2} & if\ W_{(t-1)} > 0 \\ T_{(t)} = T_{(t-1)} + 1 & if\ W_{(t-1)} = 0 \end{cases} \quad (6)$$

Finally, the simulated concentration in minute t is given by Equation (7):

$$C_{(t)} = \frac{W_{(t)}}{Q_{(t)}.60} \quad (7)$$

where $Q_{(t)}$ is the discharge [L/s].

3.2.5. Quality sensitivity analysis

The influence of warming up the model on the initial buildup was analyzed. Therefore, antecedent warm up periods (*Tw*) of 1, 2 and 6 months were used to compare the buildup at the beginning of Ev.1 and Ev.6. For this analysis, 3 different *b*2 were used (0.1, 0.05 and 0.01 days^{-1}) with 3 different *w*1 (0.5, 0.07, 0.01). Table 3.3 presents the simulation periods and their considered initial buildup.

Table 3.3: Warm up periods before Ev.1 and Ev.6.

	Tw (months)	**Warm up period**	***T (dry days)**	**Accumulated rainfall depth in the period (mm)**
Ev.1	6	02/25/2015 - 08/25/2015	30.0	626
	2	06/25/2015 - 08/25/2015	6.0	94
	1	07/25/2015 - 08/25/2015	14.0	1
	0	0	29.0	-
Ev.6	6	16/11/2015 - 16/05/2014	6.0	801
	2	16/03/2016 - 16/05/2015	0.0	41
	1	16/04/2016 - 16/05/2016	16.0	9
	0	0	0.5	-

Note: *T represents the dry period at the beginning of the warm up period

Before the quality calibration, a sensitivity analysis of the buildup and washoff parameters was also performed by varying the *w*1, *w*2, *b*1 and *b*2, to verify their influence on the concentration.

3.3. Results and discussion

3.3.1. Quantity calibration and validation

Table 3.4 presents the calibrated catchment parameters and the typical values for its soil type.

Table 3.4: Catchment parameters after quantity calibration.

PARAMETER	Used	Typical Values	Obs
Width (m)	130	NA	GIS assisted
Slope (%)	3.5	NA	GIS assisted
Imperv. (%)	22	NA	GIS assisted
N Imperv	0.017	0.011 - 0.024	Smooth asphalt - Cement rubble surfaces (McCuen, 1996)
N Perv	0.2	0.15	Short grass (McCuen, 1996)
Dstore Imperv (mm)	0.85	1.27 - 2.54	Impervious surfaces (ASCE, 1992)
Dstore Perv (mm)	3.0	2.54-5.08	Lawns (ASCE, 1992)
Suction Head (cm)	15.0	5.57-141.5 / 1.8-41.85	Sandy Clay Loam / Sandy Loam (Rawls, 1982)
Conductivity (mm/hr)	6.0	1.5/10.9	Sandy Clay Loam / Sandy Loam (Rawls, 1982)
Initial Deficit (frac.)	0.143	0.143 / 0.246	Difference between soil porosity and field capacity (Rossman, 2010). Values for Sandy Clay Loam / Sandy Loam

Note: NA = not applicable.

The quantity calibration and validation results can be observed in Table 3.5. The simulated and observed discharges in the calibration and validation are shown in Figure 3.2.

The total predicted volume for Ev.4 presented the highest variation when compared to the observed one. It was 21.20% lower, while Ev.7 was the most precise with -1.02% in the total predicted volume. The simulated peak in Ev.3 was 93.03% higher than that observed, but this event has a total predicted volume difference of only 2.96% and a satisfactory NSE value of 0.74.

Table 3.5: Quantity calibration and validation results.

	Events	NSE	R^2	*Total observed depth (mm)	*Total predicted depth (mm)	Total volume difference (%)	Max. observed Peak (L/s)	Max. predicted peak (L/s)	Max. peak difference (%)
Calibration	**Ev.1**	0.95	0.96	0.54	0.61	13.21	22.41	22.97	2.50
	Ev.2	0.75	0.78	0.28	0.29	5.45	5.00	5.23	4.58
	Ev.3	0.74	0.89	13.96	13.55	-2.96	98.38	189.90	93.03
Validation	**Ev.4**	0.80	0.81	1.51	1.19	-21.20	39.12	37.63	-3.81
	Ev.5	0.73	0.75	1.43	1.33	-6.75	11.62	12.55	8.01
	Ev.7	0.78	0.78	3.83	3.79	-1.02	38.98	** 32.77	-15.93

Note: *Volume normalized by the catchment (2.37ha) ** The maximum peak in Ev.7 was 36.81 L/s, at 11:13am. However, the peak shown in the table was registered at 14:25pm, which is correspondent to the maximum observed peak (see Figure 3.2). The observed peak at 11:12am was 36.66 L/s (0.39% lower compared to the correspondent observed peak).

The predicted runoff discharge, as shown in Figure 3.2, is more unstable than that observed with perturbations corresponding to the precipitation occurrence. The rain gauge precision may be the reason, which registers only 0.2mm when the bucket tips, after catching the corresponding volume. In Ev.2, for example, the rainfall was light and constant, not intermittent as was used for the simulations. It generates small runoff peaks, similar to the ones observed in Ev.1 after 10:19 and is more significant for smaller events.

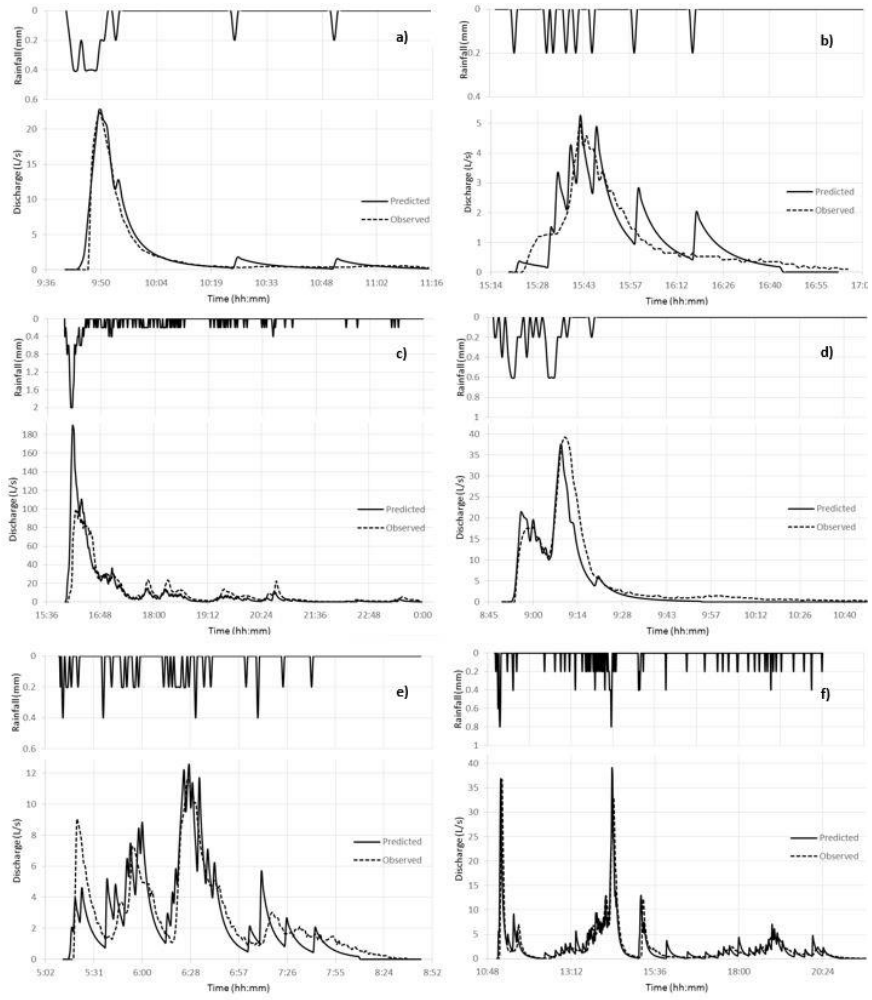

Figure 3.2: Observed and predicted runoff for: Ev.1 (a); Ev.2 (b); Ev.3 (c); Ev.4 (d); Ev.5 (e) and Ev.7 (f)

The events with qualitative monitoring are shown in Figure 3.3 and the difference between the simulated and observed runoff discharge values during the quality sampling time is visible. At 15:29, in Ev2 for example, the observed discharge was about 5 times higher, while at 16:10 in Ev.3, approximately 6 times lower. Since the discharge is crucial for representative quality modelling, the observed discharge was used for quality calibration to avoid the quantity simulation errors.

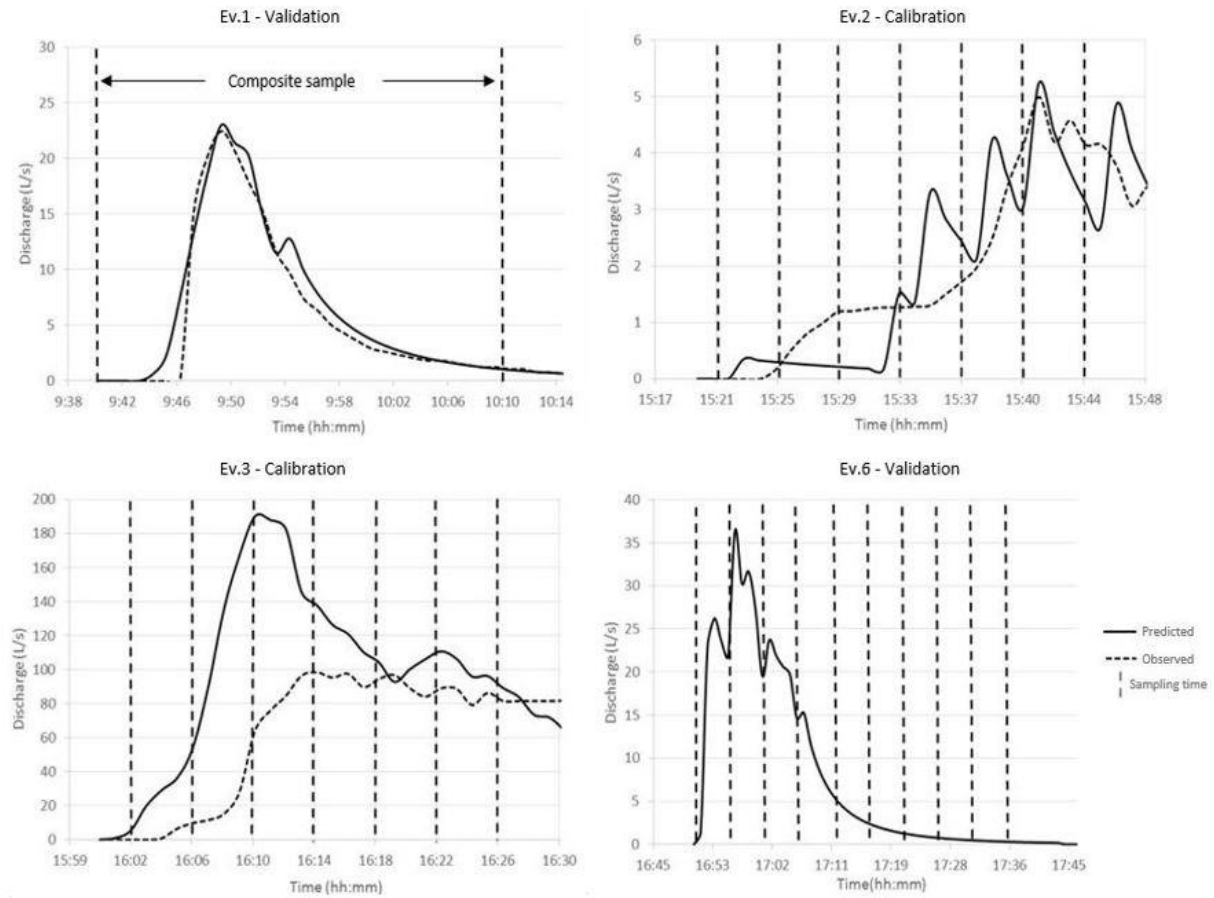

Figure 3.3: Quality monitoring events and the sampling time

3.3.2. Sensitivity analysis of the model warm up

First, the influence of the simulation period on the initial buildup was verified. Table 3.6 presents the buildup difference at the beginning of Ev.1 and Ev. 6, compared to 6 months of warm up.

Table 3.6: Buildup difference (%) relative to 6 months of warm up with sensitivity analysis of parameters *w*1 and *b*2.

		Ev.1 *b*2(1/day)			Ev.6 *b*2(1/day)		
	***Tw* (month)**	**0.01**	**0.05**	**0.1**	**0.01**	**0.05**	**0.1**
	0	-29.6	-14.1	-4.5	-93.4	-88.3	-82.8
*w*1=0.5	**1**	-2.0	0.0	0.0	-10.1	-2.3	-0.3
	2	-0.0	0.0	0.0	-0.2	-0.0	0.0
	0	-49.5	-18.6	-4.9	-89.4	-94.5	-94.9
*w*1=0.07	**1**	-44.8	-4.9	-3.4	-27.3	-6.3	-0.8
	2	-15.7	-1.3	-0.1	-12.0	-1.5	-0.1
	0	-66.6	-22.5	-5.4	-93.9	-95.7	-95.8
*w*1=0.01	**1**	-52.0	-18.9	-3.9	-47.1	-9.1	-1.0
	2	-37.2	-3.1	-0.1	-35.0	-3.9	-0.2

The difference from 6 months tends to be higher for lower buildup accumulation (*b*2) and higher washoff rates (*w*1). For a *w*1 = 0.01 and *b*2 = 0.1 days^{-1}, the buildup can be subestimated in 99.38% in Ev.6 if *Tw*=0, while for *Tw*= 1 and *Tw* =2 previous months, the error drops to 51.93% and 31.19% in Ev .1 and to 65.32% and 34.97% in Ev.6, respectively. Using the previous simulation time is more effective for Ev.6 that only has 10.8 hours of previous dry days. With a *w*1=0.07 and *b*2=0.05 days^{-1}, for example, by using *Tw* =2, the error drops from 97.23% to 1.54%.

Configuring only with previous dry days (*Tw*= 0), it is assumed that the last rainfall event washed all the pollutant, which does not necessarily occur. The longer the warm up time, the more precise the initial buildup is. Thus, to ensure better accuracy, Ev.1 Ev.2, Ev.3 and Ev.6 were simulated continuously for the quality calibration and validation, using 6 months to warm the model up.

3.3.3. Washoff and buildup sensitivity analysis

A sensitivity analysis of a general pollutant was performed, according their buildup and washoff characteristics. The maximum buildup (*b*1) sensitivity analysis was performed

(appendix A1), and the results showed that it is directly proportional to the concentrations. A $b1$=0.1 kg/ha for example, generates concentrations 10 times higher than those with a $b1$=0.01 kg/ha. Thus, this coefficient can be used to adjust the pollutant magnitude. This kind of adjustment is an advantage of the washoff exponential equation, which considers the buildup when compared to the rating curve. Washoff predictions for small catchments are reliable (Sage et al., 2015), however buildup determination is a major problem (Obropta & Kardos, 2007), and this kind of adjustment also helps calibrate the buildup more effectively.

Concerning the washoff, the $w1$ and $w2$ were also verified and are shown in Figure 3.4. Lower values of $w2$ result in higher concentrations for lower discharge. For Ev.2 and $w2$ equal to 0.7, for example, there was a peak of concentration when the runoff was minimum, and the opposite occurred when $w2$ was equal to 1.3. When $w2$ is equal to 1, the discharge does not influence the concentration. It only decreases due to the buildup consumption, otherwise it would be constant (see appendix A2).

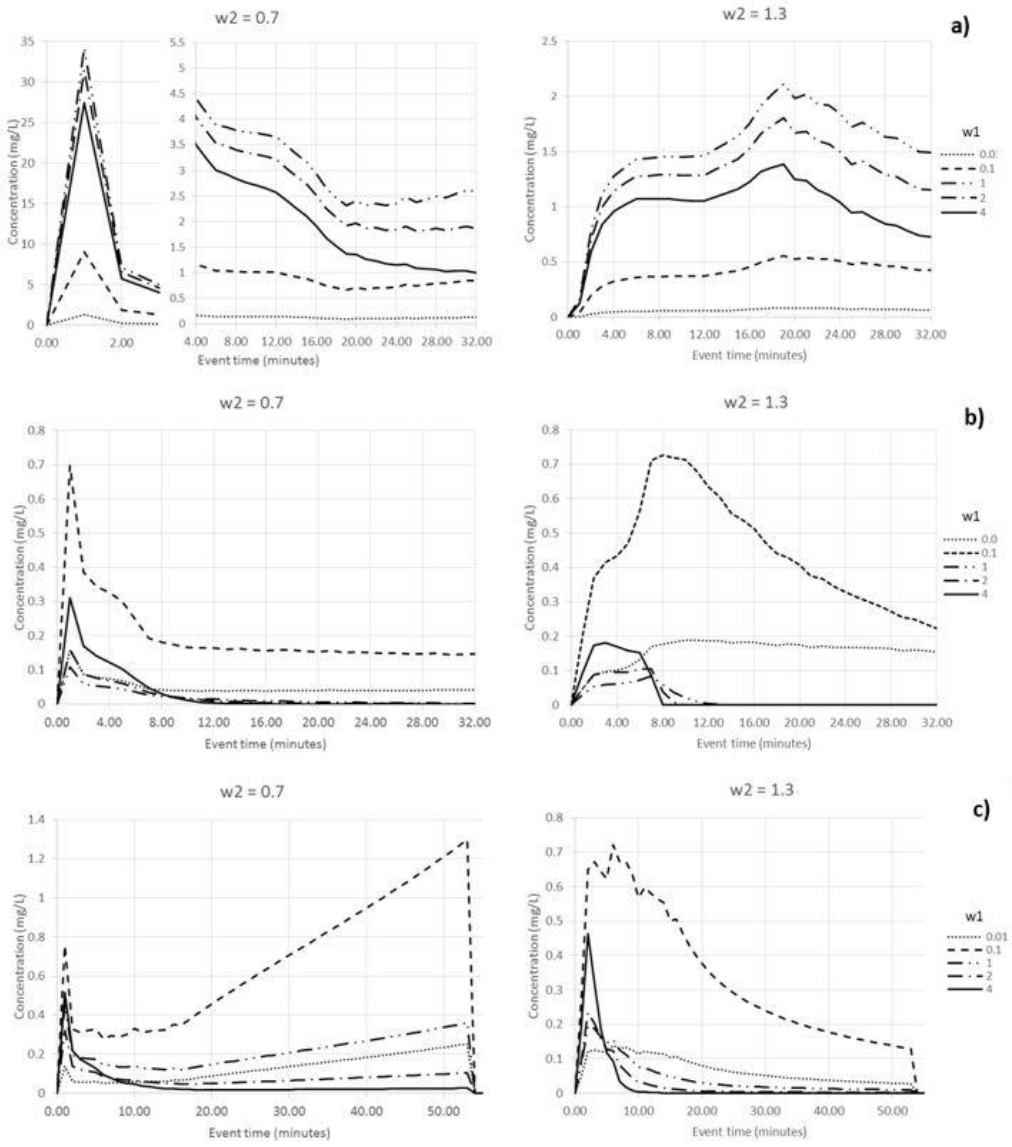

Figure 3.4: Washoff sensitivity analysis for Ev.2 (a), Ev.3 (b) and Ev.6(c). In this case, $b1$=0.1 kg/ha and $b2$=0.02 days^{-1}.

A higher $w1$ results in higher washoff values and, consequently, higher concentrations. However, the buildup decreases more rapidly and may affect the concentration as lower buildup results in lower concentrations, as previously explained. In Ev.2, the concentration increased with the $w1$ until it was equal to 1, while for Ev.3 and 4, it was until 0.1. This can be explained by the

previous rainfall events, which were less intense for Ev.2, when the highest values for *w*1 had less impact on the buildup.

For a certain value of *w*1, a previous rainfall event completely washes the pollutant off and the buildup is the same for next event, for any higher *w*1. In Ev.3 with *w*2=1.3, for instance, the initial buildup is the same for a *w*1 higher than 1. The same accumulated pollutant is washed off faster with a *w*1 equal to 4, with a higher concentration in a shorter period when compared to a *w*1 equal to 1 and 2.

This behavior concerning the *w*1 coefficient can be used to better adjustment. If the predicted concentration is too low in Ev.2 and too high in Ev.3 for example, it may become closer to the observed concentration in both events by simply raising the *w*1 coefficient. As high intensity rainfalls are common in the tropics, this kind of adjustment may be common and has to be considered when calibrating. It also highlights the importance of warming the model up.

Figure 3.5 shows how *w*1 influences the buildup. For lower *w*1, such as 0.01, the buildup tends to be more constant, while for a value equal to 2, the buildup ends more easily. At the beginning of Ev.3 and Ev.6, the disposal buildup is nearly null with a *w*1=1 and 2, illustrating why the concentration is lower in these events with higher *w*1 values.

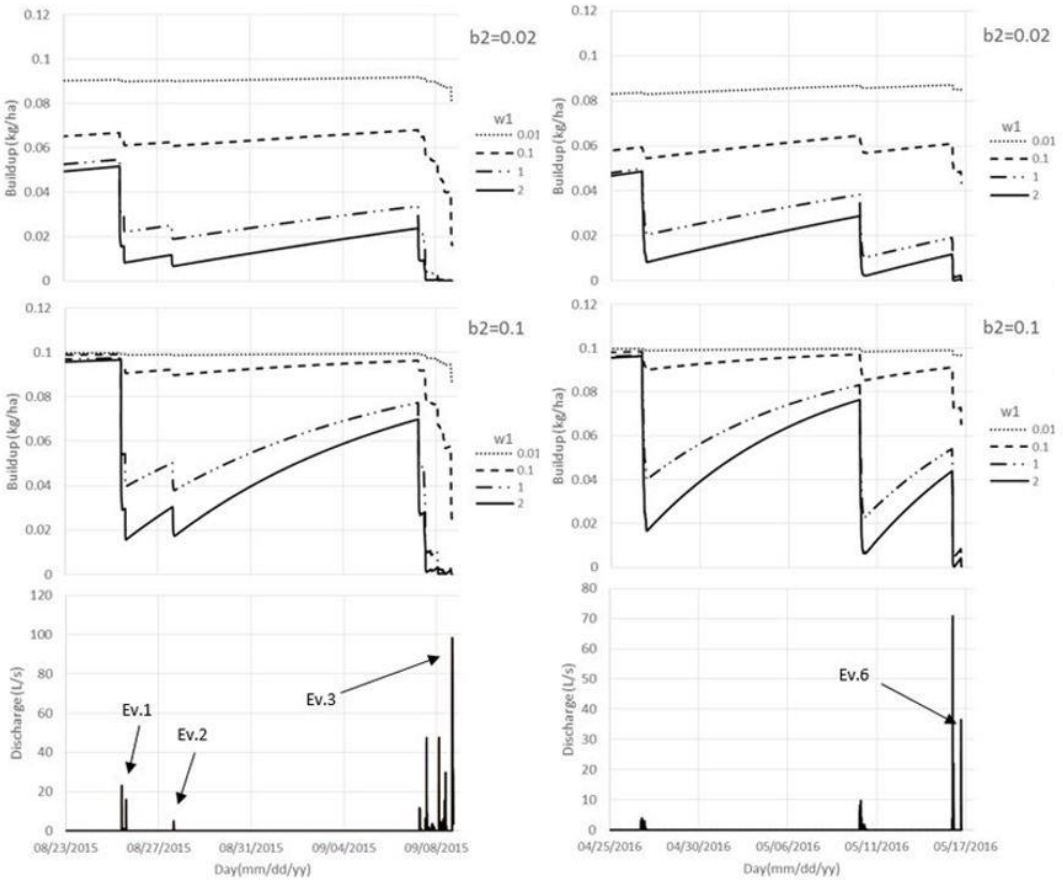

Figure 3.5: Disposal buildup decrease with runoff occurrence (influenced by *w*1) and increase (influenced by the *b*2). In this case, *b*1=0.1 kg/ha.

The influence of the buildup accumulation rate is also shown in Figure 3.5. The lower the rainfall volume prior to the event, the more influence this coefficient has on the concentrations. It can be observed in the figure that for Ev.2 with *w*1 = 1 for example, it has an initial buildup of approximately 0.25 kg/ha for *b*2 equal to 0.02 days^{-1}, and around 0.5 kg / ha when *b*2 is 0.1 days^{-1}, an increase of 100%. Regarding Ev.3, the buildup is approximately 0.006 and 0.028 kg / ha for *b*2 equal to 0.02 and 0.1 days^{-1} respectively, representing an increase of 330%.

3.3.4. Quality calibration and validation

The buildup and washoff parameters after the concentration and load-based calibration are presented in Table 3.7.

Table 3.7: Calibrated buildup and washoff

	Concentration calibration				Load-based calibration			
	Washoff		Buildup		Washoff		Buildup	
	*w*1	*w*2	*b*1 (kg/ha)	*b*2 (1/days)	*w*1	*w*2	*b*1 (kg/ha)	*b*2 (1/days)
Cd	0.023	1.3	0.031	0.012	0.017	1.31	0.023	0.089
COD	0.17	0.88	8.6	0.0058	0.018	0.69	11	0.027
Fe	0.42	0.89	0.36	0.086	0.36	0.67	0.36	0.029
NH_4	0.10	0.93	0.15	0.017	0.0025	0.79	2.7	0.014
NO_3	0.29	0.92	0.10	0.024	0.011	0.45	0.82	0.0078
NO_2	0.043	0.92	0.020	0.0014	0.0012	0.86	0.080	0.024
TOC	0.062	0.92	5.9	0.0043	0.051	0.91	5.5	0.0046
PO_4	0.088	1.0	0.019	0.039	0.12	1.07	0.012	0.033
Zn	0.11	1.0	0.021	0.029	0.098	1.04	0.021	0.029

Table 3.8 compares the predicted and observed results for the calibration (Ev.2 and Ev.3) and validation (Ev.6). The concentration-based calibration, as expected, resulted in predicted concentrations close to those observed, except for Fe in Ev.3 with a variation of 193% in the mean concentrations. NH_3 , Cd, COD and Fe did not have the same proximity in the concentrations for Ev.6 with a variation of 164, 574, 193, 226%, respectively. In Ev.1, the highest variation was determined for Fe, when the predicted concentration was 45.9% higher, indicating that this calibration was suitable in this event.

The load-based calibration generally resulted in a higher variation in the mean concentration, such as NO_3 in Ev.2 with a 214% variation against 16.4% when calibrating the concentration. However, this method more accurately predicted the total pollutant mass, and consequently the event mean concentration (EMC) since the runoff volume is constant. Even with a 214% variation in NO_3 mean concentration, the predicted total mass was only 1.9% lower, while the predicted mass, using the concentration-based calibration, was 52% higher. The

validation with Ev.1 presented good results, except for Fe with 80% variation. The mass variation was also low in Ev.6, indicating a good fit of the calibrated buildup and washoff parameters.

Table 3.8: Calibration methods comparison.

		Concentration-based calibration		Load-based calibration	
		Difference of mean concentration (%)	**Difference of EMC/total mass (%)**	**Difference of mean concentration (%)**	**Difference of EMC/total mass (%)**
Cd	Ev.1	38.39	-	13.00	-
	Ev.2	-5.13	10.09	-22.72	-10.31
	Ev.3	3.46	11.88	-14.56	-7.34
	Ev.6	573.73	775.20	510.72	691.86
COD	Ev.1	4.51	-	-35.14	-
	Ev.2	17.27	37.09	7.20	-11.35
	Ev.3	-15.79	-10.42	-21.54	-23.74
	Ev.6	192.69	128.99	238.84	63.57
Fe	Ev.1	45.92	-	80.28	-
	Ev.2	-10.29	8.33	8.95	-15.09
	Ev.3	192.68	101.17	62.79	-1.49
	Ev.6	226.39	49.56	199.85	-19.75
NH_4	Ev.1	-29.29	-	-29.29	-
	Ev.2	4.23	21.13	-109.48	-9.71
	Ev.3	-5.60	-7.02	109.53	-19.21
	Ev.6	163.78	126.60	-45.33	86.09
NO_3	Ev.1	17.45	-	1.92	-
	Ev.2	16.40	51.62	214.27	-1.88
	Ev.3	2.66	18.50	13.47	-10.02
	Ev.6	28.19	26.71	171.53	-19.92
NO_2	Ev.1	24.29	-	24.29	-
	Ev.2	-15.32	-1.69	-14.79	-7.41
	Ev.3	-4.61	-0.29	-8.14	-5.95
	Ev.6	-10.17	-59.90	15.27	-8.80
TOC	Ev.1	0.90	-	12.36	-
	Ev.2	-10.57	-2.13	-14.91	-7.82
	Ev.3	-10.67	-1.22	-12.93	-3.86
	Ev.6	9.18	20.55	4.99	13.36
PO_4	Ev.1	-2.31	-	4.55	-
	Ev.2	7.99	11.72	-7.24	-1.24
	Ev.3	3.50	18.69	-19.69	-7.86
	Ev.6	14.08	12.08	-11.24	-4.36
Zn	Ev.1	12.41	-	12.84	-
	Ev.2	0.27	1.38	-7.61	-5.39
	Ev.3	-4.71	-6.44	-2.34	-2.99
	Ev.6	16.59	0.45	11.48	-1.04

The only pollutants with high mass variation were NH_3, Cd, and COD, in which the observed concentrations were too low. Other attempts to adjust the predicted concentrations to

the observed ones in this event were made, such as a higher *w*1 coefficient for a lower initial buildup in this event or a lower *b*1. However, the good fit in Ev. 2 and/or Ev. 3 were lost, suggesting that this model was not good for these pollutants prediction.

Figure 3.6 shows the calibration methods for PO_4 in Ev.3. By optimizing the NSE of the load pollutograph, the fit of concentrations in higher runoff discharges is prioritized. The first two samples pull the calibration upwards when the concentration is calibrated. By calibrating the load, these two samples tend to be ignored for a closer approximation of the following samples, when the discharge is considerably higher. The calibration and validation of the other pollutants can be observed in the appendix (appendix Figures A4-A12).

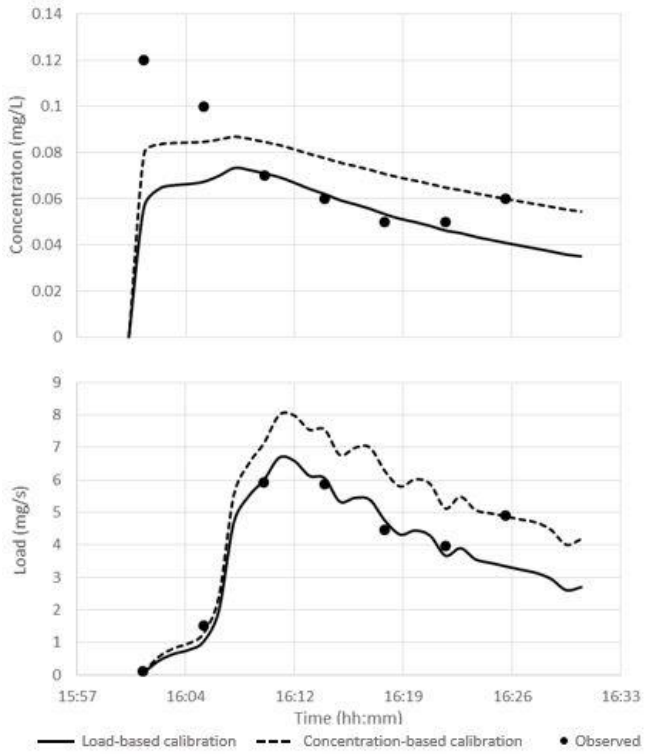

Figure 3.6: PO_4 calibration in Ev.3

As this study aims to estimate the total mass of pollutants and their EMCs into the bioretention, and not to analyze the distribution of concentrations over time as first flush studies, the load-based calibration method was used for the simulations. Since NH_4, Cd, and COD could not be validated with Ev.6, they were not included in the simulations to characterize the runoff in this study. However for the other pollutants, this kind of calibration also generated satisfactory values of VE, NSE and R^2 for their load pollutograph (appendix Table A3), in addition to the predicted mass proximity.

3.3.5. Runoff characterization

First, rainfall events were separated by duration or, for those without runoff, by the basin time of concentration of 20 minutes. A total of 1,520 events occurred in the period, of which 628 (41%) did not generate runoff with a total rainfall varying from 0.2mm and 0.8mm. Every event with 1mm or higher generated runoff.

Table 3.9 presents the predicted runoff volume and the total mass of Fe, NO_3, NO_2, PO_4, TOC and Zn. Over 4 years, approximately 1223mm (or 29.000m^3) of runoff was generated. This runoff washed approximately 9659g/ha, 3818.2g/ha, 93.8g/ha, 306.9g/ha, 29731g/ha, 475.5g/ha of Fe, NO_3, NO_2, PO_4, TOC and Zn, respectively, per hectare of catchment.

The proportion of washed pollutants was also observed in the seasons. As expected, summer is the season when the highest mass of pollutants is washed, followed by spring, autumn and winter, a result influenced mainly by the total volume of rainfall. The only exception is TOC, which was more washed in spring than summer, and more in winter than autumn, influenced maybe by the leaves falling during the winter. The proportions of NO_2 throughout the seasons are the most similar to the proportions of runoff, suggesting that this pollutant washing is more dependent on the runoff.

Table 3.9: Predicted runoff quality and quantity for the simulated period (March, 2013- March, 2017)

	Rainfall	Runoff	Fe	NO3	NO2	PO4	TOC	Zn
				Absolute values				
	(mm)	(mm)	(g/ha)	(g/ha)	(g/ha)	(g/ha)	(g/ha)	(g/ha)
Total accumula	4644.2	1223	9659	3818.2	93.8	306.9	29731	475.5
Year averag	1161 (±208)	305.8 (±9.5	5723 (±687)	2262 (±271)	55.5 (±13.9	181.8 (±8.8	17615 (±757)	281.6 (±10.5)
				Seasonal fraction (%)				
Autumn	16.39%	14.60%	19.95%	15.59%	14.89%	18.76%	17.83%	18.73%
Winter	7.64%	7.75%	16.93%	10.11%	7.95%	14.94%	19.06%	15.21%
Spring	30.96%	31.95%	30.70%	35.58%	32.15%	31.46%	35.20%	31.71%
Summer	45.01%	45.70%	32.42%	38.73%	45.01%	34.84%	27.91%	34.36%

A relation between the total runoff volume and pollutant mass generated in an event was observed and is shown in Figure 3.7. It can be observed that for lower *w*1, the relation between the runoff volume and pollutant mass was more linear as it had a lower impact on the total buildup, as can be seen in the section on washoff and buildup sensitivity analysis. This explains the similarity in runoff and NO_2 proportion in the seasons. This influence of the *w*1 on relation between total pollutant mass and total runoff volume is expected be more significant in the tropical zone, due to higher frequency of intense rainfalls.

For Zn, PO_4 and Fe, the event that generated the highest mass was a 29.6mm rainfall depth that generated 171.3m³ of runoff. It was the first rainfall event with runoff in the spring of 2016, after a winter with only 5.2mm of rainfall.

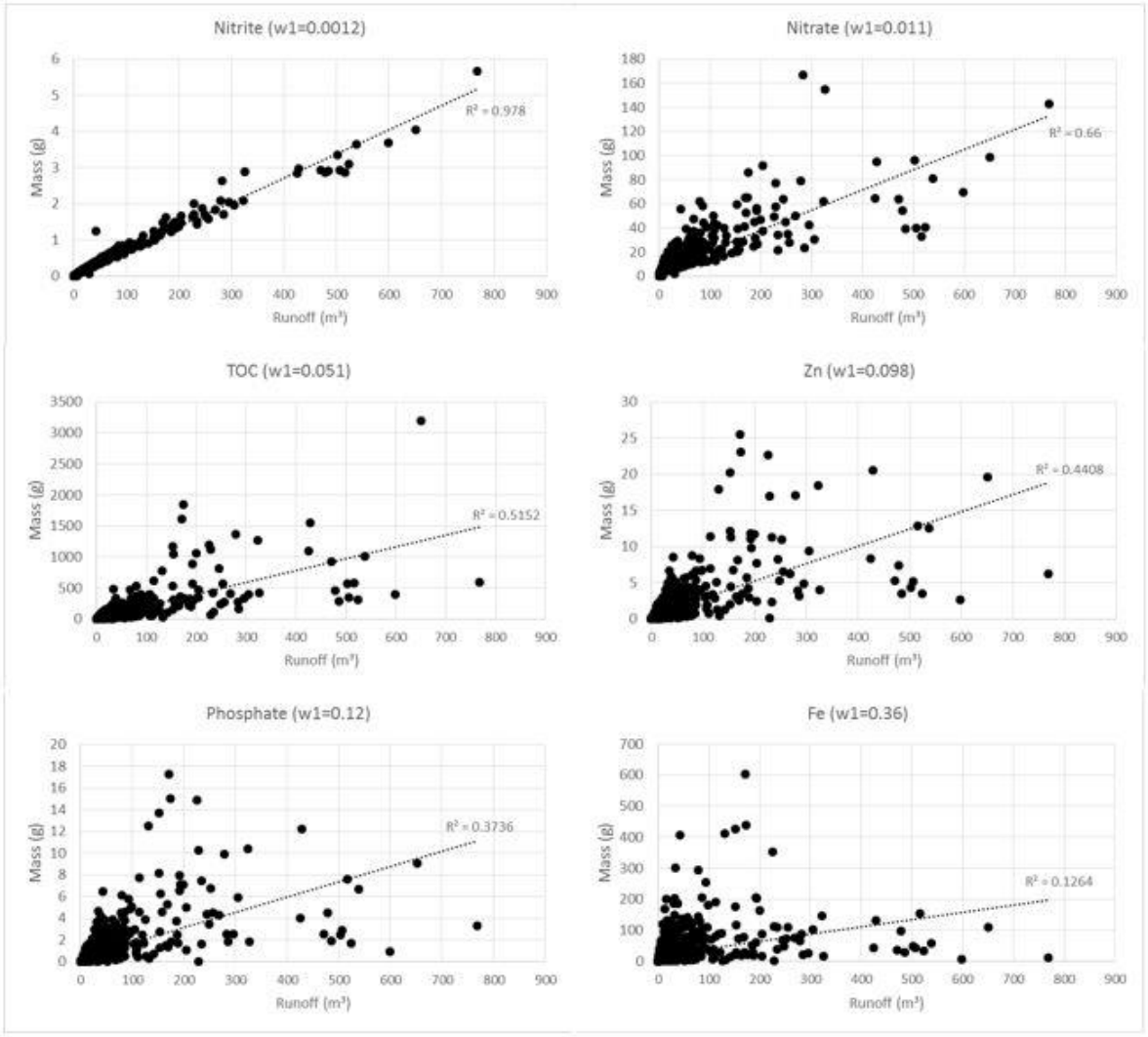

Figure 3.7: Runoff volume and pollutant mass relation

The EMC for each of these events was calculated and their mean for each one was determined, shown in Table 3.10. In general, the highest EMCs were found during the winter, followed by autumn, spring and summer, except for NO_3 that has an EMC in spring higher than in autumn. It occurs due to longer accumulation periods and lower runoff volumes during the winter, facilitating the buildup increase. Winter is also the season when water bodies have lower discharges and higher concentrations of pollutants in the runoff can be more harmful.

Table 3.10: Predicted EMC of the pollutants

	Fe (mg/L)	NO_3 (mg/L)	NO_2 (mg/L)	PO_4 (mg/L)	TOC (mg/L)	Zn (mg/L)
Autumn	2.84 (±3.57)	1.09 (±0.81)	0.011 (±0.0026)	0.036 (±0.029)	3.65 (±2.33)	0.055 (±0.042)
Winter	6.05 (±6.17)	1.53 (±0.84)	0.012 (±0.0020)	0.059 (±0.037)	7.25 (±2.79)	0.092(±0.051)
Spring	2.25 (±2.41)	1.32 (±0.94)	0.011 (±0.0023)	0.031 (±0.0023)	3.43 (± 2.15)	0.048 (±0.033)
Summer	1.70 (±2.01)	0.98 (±0.73)	0.011 (±0.0032)	0.026 (±0.019)	2.36 (±1.42)	0.040 (±0.027)
Total period	2.46 (±3.27)	1.15 (±0.83)	0.011 (±0.0028)	0.032 (±0.026)	3.34 (±2.40)	0.050 (±0.038)

The predicted EMCs found in this study are relatively low when compared to other runoff EMCs found in literature (Table 12), which indicates that the studied catchment presents low contaminant content. The average EMC of Nitrite, phosphate, TOC and Zn lower than any of those presented in table 12, while Fe was higher when compared to the one found by Bäckström et.al (2003) and nitrate when comparing to Wang et. al (2013), Zhang et.al (2012) and Barrett et.al (1998). The pollutants concentration in the runoff vary from each study presented in the table, and those with the same catchment type have also different EMCs. The reason may be other influencing factors such as soil type and pollution sources at the surroundings.

This studied catchment is surrounded by an environmental conservation area, which may prevent higher pollutants buildup in the area. Another possible reason to low EMC is the fact of including all the events in the entire period, even the ones after other events when the buildup is relatively lower.

Table 3.11: Average EMC in other studies

		EMC (mg/L)						
Location	**Catchment type**	**Fe**	**NO_3**	**NO_2**	**PO_4**	**TOC**	**Zn**	**Reference**
China	University Campus	11.8	1	-	-	-	0.69	Wang et.al (2013)
China	Farmland	-	4.18	-	0.32	-	-	Lang et.al (2013)
	Forestland	-	0.6	-	-	10.3	-	
China	Farmland	-	5.09	-	-	19.7	-	Zhang et.al (2012)
	Village	-	9.9	-	-	10.8	-	
USA	Parking lot	-	0.39	0.025	0.075	12	-	Brown & Borst (2015)
USA	Highway	2.8	1.07	-	-	46	0.22	Barrett et.al (1998)
Sweden	Highway	0.33	2.87	-	-	11.8	0.13	Bäckström et.al (2003)
USA	Highway	-	2.7	0.3	0.2	-	0.5	Han et.al (2006)
Italy	Highway	3.1	4.8	0.7	-	-	1.7	Mangani et.al (2005)
Germany	Roof	-	-	-	-	4.3	6.8	Schriewer et.al (2008)

3.4. Conclusions

This paper discussed the steps to estimate the quantity and quality of runoff drained in the past 4 years in a subtropical catchment. Firstly, a sensitivity analysis elucidated how the buildup and washoff parameters influence the predicted concentration: (i) buildup estimation can be easier when using washoff exponential equation, rather than the rating curve; (ii) the magnitude of concentration can be also adjusted with the *w*1, when combined to previous rainfall characteristics; (iii) the calibration reliability of events were highly dependent upon the model warm-up period.

Concerning the model calibration and validation, the following can be summarized: (i) the overall calibration and validation of the quantity was satisfactory. The higher difference in peak flows was for Ev.3, in which the predicted peak was 93% higher. Ev.4 presented the highest difference in the total runoff volume, and the simulated one was approximately 20% lower. (ii) the quality load-based calibration presented a greater proximity of the total mass and the EMC, however with a higher difference in the mean concentrations. Even with lower precision for the smallest discharge, the load-based calibration was chosen for the simulations; (iii) load-based

calibration generated satisfactory predicted pollutant mass for all pollutants with a major difference for NH_3 in Ev.3 when the predicted pollutant mass was 19% lower. However, NH_3, Cd and COD could not be validated, which suggests that the quality model used in this paper was not suitable for these pollutants.

After quality and quantity calibration and validation, the runoff could be finally characterized: (i) in 4 years, it is estimated that 9659g/ha, 3818.2g/ha, 93.8g/ha, 306.9g/ha, 29731g/ha, 475.5g/ha of Fe, NO_3, NO_2, PO_4, TOC and Zn were respectively washed by approximately 1223 mm (or 29,000m^3) of runoff; (ii) the lower the $w1$ coefficient, the more linear the relation between the total pollutant mass generated and the total runoff; (iii) except for TOC, most of the pollutant mass was generated during the summer (wet season). Winter (dry season) presented the highest EMCs, followed by Autumn (post dry season), due to longer accumulation periods.

3.5. References

American Society of Civil Engineers (ASCE) and the Water Environment Federation (WEF), 1992. *Design and Construction of Urban Stormwater Management Systems. ASCE Manuals and Reports of Engineering Practice No. 77*, WEF Manual of Practice FD-20

APHA. (2005). Standard Method for Water and Wastewater Examination, 17th edn. American Public Health Association, Washington, D.C.

Bäckström, M., Nilsson, U., Håkansson, K., Allard, B., & Karlsson, S. (2003). Speciation of heavy metals in road runoff and roadside total deposition. *Water, Air, & Soil Pollution*, *147*(1), 343-366.

Barrett, M. E., Irish Jr, L. B., Malina Jr, J. F., & Charbeneau, R. J. (1998). Characterization of highway runoff in Austin, Texas, area. *Journal of Environmental Engineering*, *124*(2), 131-137.

Bertrand-Krajewski, J. L. (2007). Stormwater pollutant loads modelling: epistemological aspects and case studies on the influence of field data sets on calibration and verification. *Water Science and Technology*, *55*(4), 1-17.

Bonhomme, C., & Petrucci, G. (2017). Should we trust build-up/wash-off water quality models at the scale of urban catchments?. *Water research*, *108*, 422-431.

Borah, D. K. (2011). Hydrologic procedures of storm event watershed models: a comprehensive review and comparison. *Hydrological Processes*, *25*(22), 3472-3489.

Brown, R. A., & Borst, M. (2015). Nutrient infiltrate concentrations from three permeable pavement types. *Journal of environmental management*, *164*, 74-85.

Criss, R. E., Winston, W. E. (2008). "Do Nash values have value? Discussion and alternate proposals." *Hydrological Processes*, 22(14), 2723–2725.

Fletcher, T. D.; Andrieu, H.; Hamel, P. Understanding, management and modelling of urban hydrology and its consequences for receiving waters: A state of the art. *Advances in Water Resources*, v. 51, p. 261-279, 2013.

Guan, M., Sillanpää, N., & Koivusalo, H. (2015). Modelling and assessment of hydrological changes in a developing urban catchment. *Hydrological Processes*, *29*(13), 2880-2894.

Han, Y., Lau, S. L., Kayhanian, M., & Stenstrom, M. K. (2006). Characteristics of highway stormwater runoff. *Water Environment Research*, *78*(12), 2377-2388.

Lang, M., Li, P., & Yan, X. (2013). Runoff concentration and load of nitrogen and phosphorus from a residential area in an intensive agricultural watershed. *Science of the Total Environment*, *458*, 238-245.

Le, S. H., Chua, L. H. C., Irvine, K. N., & Eikaas, H. S. (2017). Modeling washoff of total suspended solids in the tropics. *Journal of Environmental Management*, *200*, 263-274.

Liu, J.; Sample, D. J. ; Owen, J. S. ; Li, J. ; Evanylo, G. (2014). Assessment of selected bioretention blends for nutrient retention using mesocosm experiments. *Journal of Environmental Quality*, 43(5), 1754-1763.

Macedo, M. B., Rosa, A., do Lago, C. A. F., Mendiondo, E. M., & de Souza, V. C. B. (2017). Learning from the operation, pathology and maintenance of a bioretention system to optimize urban drainage practices. *Journal of Environmental Management*, *204*, 454-466.

Mangani, G., Berloni, A., Bellucci, F., Tatàno, F., & Maione, M. (2005). Evaluation of the pollutant content in road runoff first flush waters. *Water, Air, & Soil Pollution*, *160*(1), 213-228.

McCuen, R. H., Johnson, P. A., and Ragan, R. M. (1996). *Highway hydrology, hydraulic design series No. 2.* FHWA-SA-96-067, Federal Highway Administration, Washington, D.C.

Miranda, M. J., Pinto, H. S., Zullo Júnior, J., Fagundes, R. M., Fonsechi, D. B., Calve, L., & Pellegrino, G. Q. (2012). Clima dos municípios paulistas. *CEPAGRI Meteorologia UNICAMP. Available at: http://www. cpa. unicamp. br/outras-informacoes/clima-dos-municipios. Acessed 07/20/2017*.

Nash, J. E., & Sutcliffe, J. V. (1970). River flow forecasting through conceptual models part I—A discussion of principles. *Journal of hydrology*, *10*(3), 282-290.

Obropta, C. C., & Kardos, J. S. (2007). Review of urban stormwater quality models: deterministic, stochastic, and hybrid approaches. *JAWRA Journal of the American Water Resources Association*, *43*(6), 1508-1523.

Rawls, W. J., Brakensiek, D. L., & Saxtonn, K. E. (1982). Estimation of soil water properties. *Transactions of the ASAE*, *25*(5), 1316-1320.

Rode, M., Arhonditsis, G., Balin, D., Kebede, T., Krysanova, V., Van Griensven, A., & Van der Zee, S. E. (2010). New challenges in integrated water quality modelling. *Hydrological processes*, *24*(24), 3447-3461.

Rosa, A. (2016). *Bioretention for diffuse pollution control in SUDS using experimental-adaptative approaches of ecohydrology*. PhD Thesis. School Of Engineering At São Carlos, University Of São Paulo, São Carlos, Brazil.

Rossman, L. A. (2010). *Storm water management model user's manual, version 5.0* (p. 276). Cincinnati, OH: National Risk Management Research Laboratory, Office of Research and Development, US Environmental Protection Agency.

Sage, J., Bonhomme, C., Al Ali, S., & Gromaire, M. C. (2015). Performance assessment of a commonly used "accumulation and wash-off" model from long-term continuous road runoff turbidity measurements. *Water research*, *78*, 47-59.

Schriewer, A., Horn, H., & Helmreich, B. (2008). Time focused measurements of roof runoff quality. *Corrosion Science*, *50*(2), 384-391.

Sillanpää, N., & Koivusalo, H. (2015). Stormwater quality during residential construction activities: influential variables. *Hydrological Processes*, *29*(19), 4238-4251.

Soil Science Division Staff. (2017). Soil survey manual. C. Ditzler, K. Scheffe, and H.C. Monger (eds.). *USDA Handbook 18*. Government Printing Office, Washington, D.C.

Sun, S., Barraud, S., Branger, F., Braud, I., & Castebrunet, H. (2017). Urban hydrologic trend analysis based on rainfall and runoff data analysis and conceptual model calibration. *Hydrological Processes*, *31*(6), 1349-1359.

Sun, Y., Tong, S., & Yang, Y. J. (2016). Modeling the cost-effectiveness of stormwater best management practices in an urban watershed in Las Vegas Valley. *Applied Geography*, *76*, 49-61.

Taffarello, D, Mohor, G S, Calijuri, MC, Mendiondo, E M (2016): Field investigations of the 2013–14 drought through qualiquantitative freshwater monitoring at headwaters of Cantareira System, Brazil, Water International, DOI: 10.1080/02508060.2016.1188352

Taffarello, D., Srinivasan, R., Mohor, G. S., Guimarães, J. L. B., Calijuri, M. D. C., & Mendiondo, E. M. (2017): Modelling freshwater quality scenarios with ecosystem-based adaptation in the headwaters of the Cantareira system, Brazil, *Hydrol. Earth Syst. Sci.*

Wang, S., He, Q., Ai, H., Wang, Z., & Zhang, Q. (2013). Pollutant concentrations and pollution loads in stormwater runoff from different land uses in Chongqing. *Journal of Environmental Sciences,* 25(3), 502-510.

Zhang, W. S., Wang, X. Y., Li, X. X., Ren, W. P., & Li, J. H. (2012*).* Diffuse export of nutrients under different land uses in the irrigation area of lower Beiyunhe River (China). *Procedia Environmental Sciences, 13, 1363-1372. Discuss*., https://doi.org/10.5194/hess-2017-474, in review.

Zaffani, A G, Cruz N, Taffarello, D, Mendiondo, E M (2015) Uncertainties in the Generation of Pollutant Loads using Brazilian Nested Catchment Experiments under Change of Land Use & Land Cover. J. Phys Chem Biophys, DOI: 2015.10.4172/2161-0398.1000e123

4. EFFECTS OF CLIMATE CHANGE ON LOW IMPACT DEVELOPMENT (LID) PERFORMANCE - A CASE STUDY IN SÃO CARLOS, BRAZIL.

A modified version of this chapter will be submitted as: César Ambrogi Ferreira do LAGO et al., Effects of Climate Change on Low Impact Development (LID) Performance - a Case Study in Sao Carlos, Brazil.

Abstract

Urbanization increases runoff volume and velocity, resulting in higher risks of flooding and a higher amount of pollutants carried by stormwater. To mitigate these impacts, Low Impact Development practices (LID), such as bioretention have been used to treat stormwater runoff enhancing the sustainability of urban drainage systems. However, climate change is expected to alter the rainfall regime and, consequently, the efficiency of LID controls, and its impacts need to be better evaluated. In addition, there are few studies analyzing LID performance under a subtropical climate, which has different rainfall regimes and a runoff generation process when compared to temperate climates. This study, in particular, estimated the efficiency of a bioretention in São Carlos, Brazil in a subtropical region for 4 different future periods (2020-2039, 2040-2059, 2060-2079 and 2080-2099) with an estimated rainfall for 2 RCP scenarios (4.5 and 8.5), forced by the HADGEM2-ES global model. These scenarios were based on the ETA Regional Climate model and downscaled to São Carlos by the Brazilian National Institute for Space Research and compared to the period of 1980-1999. The PCSWMM software was used to determine the income of runoff and pollutants and a specific model for the outflow was used to better represent the characteristics of the studied bioretention. In 100 years, the precipitated volume will decrease by 13% and 29% if RCP 4.5 or RCP 8.5 occur, respectively. Climate change, however has little effect on the quantity efficiency, which is approximately 80% for both scenarios and all analyzed periods. Climate change improves the EMC reduction by the bioretention, minimizing the EMC increase by the phenomenon. Results show that pollutants with higher w1 washoff coefficient will have higher EMC reduction over the years. The bioretention efficiencies tend to maintain over the years. On the other hand, the EMC reduction tends to increase.

Keywords: Climate changes, Bioretention, Quali-quantity efficiencies.

4.1.Introduction

According to IBGE (2016), approximately 185 million Brazilians live in urbanized areas. One of the main consequences of urban development is the change in the hydrologic cycle as it generates soil imperviousness, resulting in an increase in the runoff volume (Lucas & Sample 2015, Guan, Sillanpää, & Koivusalo, 2015), and consequently in higher risks of floods (Sun, Tong & Yang 2016, Sun et al. 2017) and the amount of pollutants carried (Flecther, Andrieu & Hamel, 2013), affecting the quality of urban rivers. Thus, poorly planned urbanization tends to increase qualitative and quantitative water insecurity. To mitigate these impacts, Low impact Developments (LID), such as bioretention cells are being used to treat not only quantitative but also qualitative rainwater for a more sustainable urban drainage system (Macedo, 2017).

In addition to the influence of urbanization, different climates generate different hydrological responses that may interfere with the performance of these LID practices. In tropical climates for example, high intensity rainfalls result in a faster response in the runoff (Piro & Carbone, 2014), where the pollutants are washed faster. However, few studies evaluate LID response to the rainfall regime in these regions (Macedo et al, Submitted).

According to Marengo & Ambrizzi (2014), climate change can also aggravate water insecurity in Brazil, through greater occurrences of floods and droughts, generating various negative impacts such as the increase of food and energy insecurity. Chou et al. (2014-a) verified the impacts of climate change in South America through two Representative Concentration Pathway (RCP) scenarios of 4.5 and 8.5, forced by two global models (HadGEM2-ES and the MIROC5). They estimate that during the summer there will be a decrease in rainfall volume in the central region of Brazil and an increase in the southeast region. In the austral winter, a decrease is expected in both regions. They also suggest that intense rainfall will be more frequent

in the south-central region of the country, there will be more consecutive dry days in the northeast region, which already suffers from severe droughts, and the humid Amazon region will have fewer consecutive wet days. Lyra et al (2017) evaluated the impacts of climate change on the metropolitan areas of São Paulo, Rio de Janeiro and Santos, which are of vital economic importance to Brazil. It is estimated that there will be an average increase of 9ºC by the end of the century, if scenario RCP 8.5 prevails, with a reduction of 50%, 45% and 40% in rainfall volumes for the metropolitan region of Rio de Janeiro, Santos and São Paulo, respectively. The RCP 8.5 and 4.5 scenarios are projections of radiative forcing levels reaching respectively 8.5 and 4.5 W/m² by the end of the century based on greenhouse gas emissions (Van Vuuren, 2011).

The present study aims to evaluate the impacts of climate change on a bioretention located in the city of São Carlos, in the southeastern region of Brazil with a subtropical climate. The RCP 4.5 and 8.5 scenarios were analyzed, with downscaling based on the Eta Regional Climate Model forced by the global HadGEM2-ES model. The data were acquired with a spatial scale of 5km and a 3-hour time scale, which was later reduced to 5min through a modified Bartlett-Lewis rectangular pulse model, and therefore the generation of runoff and pollutants into the bioretention could be simulated. For the bioretention outflow, a specific model was used for greater accuracy on depth accumulation on its surface.

4.2.Methodology

4.2.1.Study area and data collection

The bioretention has 60m^2 area. It has a 0.5m top layer composed by soil, and 2.7m for storage composed by gravel (0.7m) and sand (2m). This LID has undergone thorough maintenance which has increased its efficiency (Macedo et al., 1017) and will be its performance after this maintenance that will be evaluated.

The studied bioretention is located on Campus 2 at the University of São Paulo (USP), São Carlos, Brazil, with a Cfa classification according to Köppen and Geiger. It receives runoff from an area of 2.3 hectares with 22% of imperviousness. The local soil has 20% clay, 10% silt and 70% sand composition and is classified between sandy clay loam and sandy loam soils *(USDA, 2017).* Its average slope is 3.5%, obtained through Digital Elevation Model (DEM). The campus is currently under occupation and the impervious area is expected to grow, reaching 50% by 2025 and 80% by 2100 (Rosa, 2016).

Data from seven monitored events were used to calibrate the quantity and quality of the inlet runoff, however only three have quantity data after the maintenance. The outlet calibration and validation were also done with seven monitored events, with three events after the maintenance and four more recent ones. Rainfall data was obtained using a 0.2mm precision rain gauge, installed around 400m far from the bioretention. A water level sensor (HOBO Water Level U20l-02) was used to measure the water level every minute, which was then used to calculate the discharge. The following pollutants were analysed: total organic carbon (TOC), phosphate (PO_4), nitrate (NO_3), nitrite (NO_2), iron (Fe) and zinc (Zn).

4.2.2.Bioretention outflow model

The maximum storage observed during all the monitored events was 1.7m from the 2.7m possible inside the bioretention (63% of its capacity). Thus, infiltration in the upper soil layer is the only determinant factor for the bioretention quantity efficiency. The water balance in this layer is shown in Equation (1):

$$\Delta H = \left(\frac{(Qin - Qout).t}{A.\emptyset a} + P - f.t - E \right).1000 \quad (1)$$

where ΔH (m) is the variation of the level at the surface of the bioretention, *t* (s) is the timestep, Qin ($L.s^{-1}$) is the inflow, Qout ($L.s^{-1}$) surface exit flow, A (m^2) is the surface area of the bioretention, Øa is the fraction of the unoccupied surface area, f ($mm.s^{-1}$) is the infiltration rate, P (mm) is the precipitation and E (mm) is the evaporation in *t* seconds. The outflow is given by the equation of a triangular weir as a function of the surface ponding depth (Porto, 2006). If the berm height is exceeded, there will be no more ponding on the bioretention surface and the excedance is then instantly transformed into flow. The cases for the outflow of the bioretention are given by (2):

$$\begin{cases} Qout = 0 \ \ if \ H \leq h \\ Qout = 1.427(H-h)^{2.5} \ if \ H > h \\ Qout = 1.427hb^{2.5} + A.\emptyset a.(H-hb) \ if H > hb \end{cases} \quad (2)$$

for a ponding depth *H* (m), a height *h* (m) of the weir e and a *hb* (m) berm height.

The infiltration rate *f* was calculated by the Green-Ampt method (Green & Ampt, 1911), in Equation (3)

$$f = k_s \frac{(\Psi + L + H)}{L} \quad (3)$$

where k_s is the saturated hydraulic conductivity (mm/s), Ψ (mm) is the suction head and *L* (mm) is the depth of the saturated layer, given by (4). Since below the soil is a layer of gravel and a layer of sand, with a much higher hydraulic conductivity, they will not be saturated and *L* will always be equal to or lower than the soil layer depth L_s(mm).

$$L = \frac{F}{\theta_d} \quad (4)$$

$$\theta_d = (\Phi - \theta_i) \quad (5)$$

$$0 < L \leq L_s \tag{6}$$

where F (mm) is the total infiltrated depth, θ_d is the moisture deficit, Φ is the soil porosity and θ_i is the initial moisture below the wetting front, given by (4).

For values of L → 0 at the beginning of the infiltration process, $f \to \infty$. To prevent the possibility of an infinite infiltration value, the maximum depth (f_{max}) to be infiltrated in a time, correspondent to the minimum timestep, was obtained. Therefore, the maximum infiltrated depth at an event beginning must be equal to the infiltration rate:

$$f_{max} = k_s \frac{\left(\Psi + \frac{f_{max}}{\theta_d} + H\right)}{\left(\frac{f_{max}}{\theta_d}\right)} \tag{7}$$

During the phase there will be no ponding, then H=0. After working equation (7), f_{max} is given by Equation (8):

$$f_{max} = \frac{k_s \theta_d}{2}\left(\theta_d{}^{-1} + \sqrt{\theta_d{}^{-2} + \frac{4\Psi}{k_s \theta_d}}\right) \tag{8}$$

The value of θ_i, to calculate θ_d, depends on the water depth (LW) contained in the soil, by Equation (6). The maximum depth in the soil occurs when the whole layer is saturated and, to maintain the bioretention plants healthy, soil moisture will always be equal to or greater than the wilting point (WP).

$$\theta_i = \frac{Lw}{L_s} \tag{9}$$

$$L_s WP \leq Lw \leq L_s \Phi \tag{10}$$

The water variation in the soil varies as shown in Equation (11). If there has been infiltration, it will be added to the previous water content depth, considering that the infiltrated volume is equally distributed in the whole layer, and subtracting the evapotranspiration loss. For an amount of water greater than field capacity (FC), when the influence of the gravitational force occurs, the equation adapted from Rossman (2010) was used to decrease the water in the soil. Below the field capacity, the water decrease occurs only by evapotranspiration.

$$\begin{cases} Lw \leftarrow Lw + F - ET \quad if\ f > 0 \\ Lw \leftarrow Lw - \dfrac{Ls\sqrt{k_s}(\Phi - WP)\Delta t}{75} \quad if\ Lw \geq L_s FC \\ Lw \leftarrow Lw - ET \quad if\ Lw < L_s FC \end{cases} \tag{11}$$

The daily reference evapotranspiration was used for calibrating this model, which was calculated by the Penman-Monteith method at a station 6.7 km far from the bioretention, obtained from the Embrapa (Brazilian Agricultural Research Company) website. Diurnal and nocturnal evapotranspiration were considered separately, with nocturnal evapotranspiration corresponding to 14% of the daily total (Malek, 1992; De Dios et al, 2015).

4.2.3.Climate Change Scenarios

Four different future periods (2020-2039, 2040-2059, 2060-2079 and 2080-2099) were analyzed for 2 RCP scenarios (4.5 and 8.5), forced by the HADGEM2-ES global model. These scenarios were based on the ETA Regional Climate model and downscaled to São Carlos by the Brazilian National Institute for Space Research and is available at projeta.cptec.inpe.br (Chou et al., 2014-a; Chou et al, 2014-b; Lyra et al, 2017). The 1980-1999 period was used for comparison and this historical data was also acquired from the same website.

Moreover, $5km^2$ and 3 hour spatial and temporal resolution data of rainfall, evapotranspiration and temperature were acquired. As the concentration time of the studied basin is 20 min, the rainfall data had to be desegregated to a 5min timestep. Therefore, the Modified Bartlett-Lewis Rectangular Pulse Stochastic Rainfall Model was used for desegregation.

Modified Bartlett-Lewis Rectangular Pulse Stochastic Rainfall Model basically consists of 4 steps: (1) a storm starts according to the Poisson process (t,λ); (2) A random number η, with a gama distribution of mean α/ν and variance α/ν^2, is specified to each event; (3) Each rainfall has one or more cells; the secondary cells will start with the Poisson process $(t,\eta k)$, and no more cells will start after an exponentially distributed average time $(1/\eta\Phi)$; (4) each cell is a rectangular pulse with an exponentially distributed height with mean μ_x, and duration also exponentially distributed with mean $1/\eta$. Then the storm will be given by the sum of all cells, which has the frequency and characteristics determined by 6 parameters (λ, α, ν, k, μ_x and Φ). (Back et al., 2011; Rodriguez et al., 1987; Rodriguez et al., 1988)

Four years were used to calibrate the Bartlett-Lewis modified model parameters. To do this, the historical rainfall regime of a 5min timestep was aggregated to a 3 hour timestep and then desegregated. The calibration was done to approximate the observed and desegregated number of wet cells, variance, total rainfall and percentage of cells with a precipitation depth lower than 0.4mm, a depth between 0.4mm and 1mm, 1mm and 2mm, 2mm and 4mm, 4mm and 10mm, and those higher than 10mm. The model parameters were calibrated for each month individually, and therefore 12 calibrations were performed with 4 months each.

4.3.Results

4.3.1. Outflow calibration and validation

Table 4.1 shows the calibrated parameters. The local soil is classified between Sandy Clay Loam and Sandy Loam, (USDA, 2017), thus the reference values for these two types are shown. Two parameters in the table can be highlighted: the ponding area of 50% and the conductivity of 770mm/hr.

The percentage of 50% for the ponding area is justified by the berm that covers part of the bioretention surface area, and the surface area loss is due to the increase in the containment barrier at its back, one of the actions performed during maintenance in the technique (Macedo et al., 2017).

The difference between the conductivity measured in the soil and the effective conductivity in the bioretention is explained by the semi-direct injection measure, also performed during maintenance, which consists of holes in the soil layer and filled with sand. This calibration shows that the semi-direct injection was responsible for an increase in approximately 13,000% in the top layer hydraulic conductivity. Considering a conductivity of 3,600,000 mm/hr for sand, it is estimated that the injections correspond to 21% of the bioretention surface area.

Table 4.1: Calibrated bioretention parameters

Parameter	Used	Typical Values	Obs
Area (m²)	60	-	Sized
Ponding area (%)	50	-	Sized and maintenance measures
Berm height (mm)	30	-	Sized
Surface slope (%)	0	-	Sized
Weir height (m)	0	-	Sized
Soil Thickness (mm)	500	-	Sized
Porosity (volume fraction)	0.4	a)0.332-0.464 b) 0.351-0.555	a) Sandy Clay Loam b) Sandy Loam (Rawls, 1982)
Field capacity (volume fraction)	0.25	a) 0.186-0.324 b) 0.126-0.288	a) Sandy Clay Loam b) Sandy Loam (Rawls, 1982)
Wilting point (volume fraction)	0.13	a) 0.85-0.211 b) 0.031-0.159	a) Sandy Clay Loam b) Sandy Loam (Rawls, 1982)
Conductivity (mm/hr)	770	5.8	Measured
Suction Head (cm)	60	a)5.57-141.5 b) 1.8-41.85	a) Sandy Clay Loam b) Sandy Loam (Rawls, 1982)

Table 4.2 compares the simulated and observed bioretention outflows. The NSE and R2 values were satisfactory, except in event 7 with 0.32 and 0.56, respectively. Simulated and observed quantity efficiencies are close in both calibration and validation. The largest difference in efficiency is observed for event 11, despite the high values of NSE and R2. The simulated peak reduction also represents that observed well. Event 5 has the largest difference between the percentages of peak reduction, underestimating the peak reduction by approximately 17%, even this event presenting the best approximation between the quantitative efficiencies. The simulated and observed hygrograms also have similar behaviors, wh'ich can be observed in Appendix A13 and A14.

Table 4.2: Outflow calibration.

				Efficiency		Peak reduction	
		NSE	R^2	Predicted	Observed	Predicted	Observed
Calibration	Ev 4	0.76	0.69	64.4%	76.6%	32.6%	35.0%
	Ev 5	0.84	0.97	95.3%	93.6%	76.8%	59.1%
	Ev 6	0.88	0.91	77.2%	64.6%	29.4%	15.6%
	Ev 7	0.32	0.56	81.7%	85.3%	71.7%	73.6%
Validation	Ev 8	-	-	98.4%	100.0%	96.5%	100.0%
	Ev 10	0.9	0.91	95.4%	94.4%	77.5%	73.1%
	Ev 11	0.94	0.97	47.6%	34.2%	12.2%	0.3%

4.3.2. The bioretention performance

The bioretention performance was evaluated with rainfall between 2013 to 2017, covering period of data collection in the LID practice. Table 4.3 shows the inflow and outflow of pollutants. It is estimated that 1091mm of surface flow has entered the bioretention and 539mm left, representing a retention 50.6%.

Table 4.3: Bioretention performance.

	Runoff (mm)	Fe (g/ha)	NO3(g/ha)	NO2(g/ha)	PO4 (g/ha)	TOC (g/ha)	Zn (g/ha)
Inlet	1091.7	9270.7	3650.6	84.2	294.5	30747.6	455.5
Outlet	539.0	2528.1	993.7	36.8	119.2	13362.9	191.3
Period Efficiency	50.6%	72.7%	72.8%	56.3%	59.5%	56.5%	58.0%
Average efficiency of events *	76.6% (± 26.4%)	78.0% (± 25.0%)	76.9% (± 25.4%)	76.7% (± 26.1%)	77.8% (± 25.5%)	76.9% (± 26.0%)	77.5% (± 25.7%)

Note:*Disregarding the events with 100% efficiency.

TOC and Fe, also in Table 4.3, were the pollutants with a greater mass input, with approximately 30 and 9 kg/ha, while NO2 had the lowest amount washed into the bioretention with 84.2 g/ha. All pollutants have a removal efficiency greater than the quantity efficiency. Fe has the highest removal efficiency (72.7%) and the lowest NO2 with 56.3%. If the efficiency is analyzed through the average of all the events, the qualitative efficiencies of the pollutants are closer. This suggests that the pollutants present greater efficiencies for larger events, since events with higher rainfall volumes are less frequent and weigh less on average.

The quantity efficiency of the events was related to the average discharge, shown in Figure 4.1-a. The average discharge and quantitative efficiency appears to have an inverse exponential function relation. For average discharges below 1.8L/s, the quantitative efficiency was 100%. The event with the lowest quantitative efficiency of approximately 10% had an average flow rate of 102L/s. Figure 4.1-b shows the peak reduction in each event. The peak reduction percentage falls as they grow, until the peak events reach approximately 150 L/s. Events with a peak higher than that tend to have a reduction below 10%. Events with a peak lower than 6L/s tend to have a quantity efficiency of 100%, and hence, 100% peak reduction.

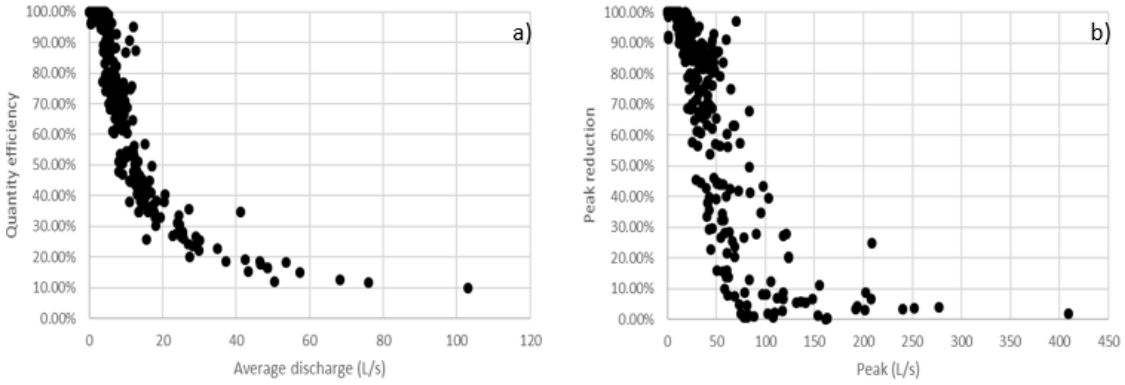

Figure 4.1: Quantity efficiency and peak reduction.

The influence of w1 and w2 of the washoff on the removal efficiency of pollutants was verified. Figure 4.2 shows that highest w1 results in the average efficiency, and the closer to 1 the value of w2 is, the more linear the relation between the qualitative and quantitative efficiency.

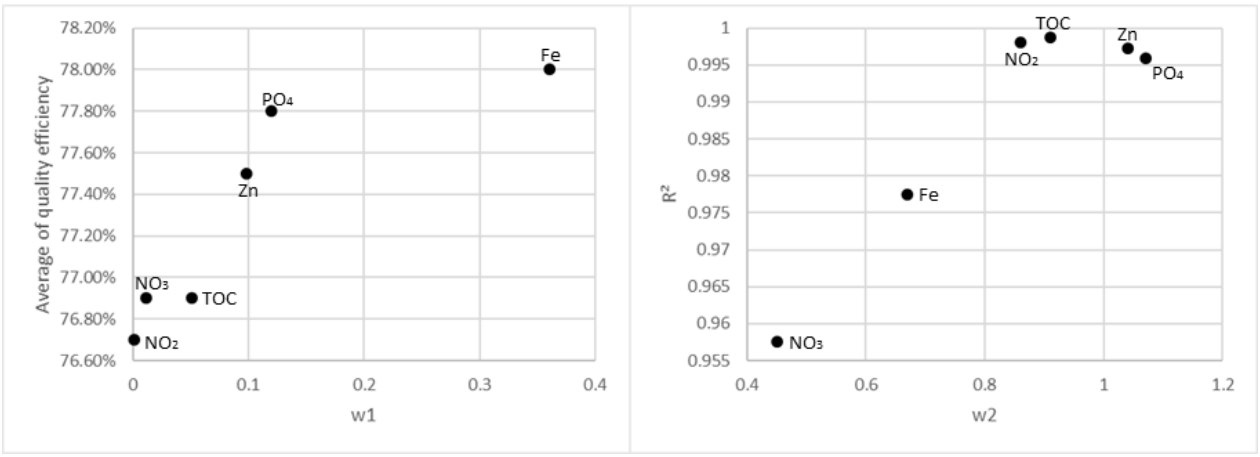

Figure 4.2: Influence of washoff parameters.

The event with the greatest difference between quantity efficiency and Fe removal, which has a higher w1, is shown in Figure 4.3 to explain why pollutants with higher w1 are better retained.

This event started with low buildup available due to previous events. The initial buildup is depleted by small discharge at the beginning of the event, as shown by the drop in concentration over the event. When Fe concentration is high, the inflow is sufficiently low for a total absorption into the bioretention, thus retaining a larger portion of the pollutant. When the inflow increases, the bioretention is not able to retain most of it, reducing the quantity efficiency. It occurs when the Fe concentration is already low, minimizing the output of the pollutant mass.

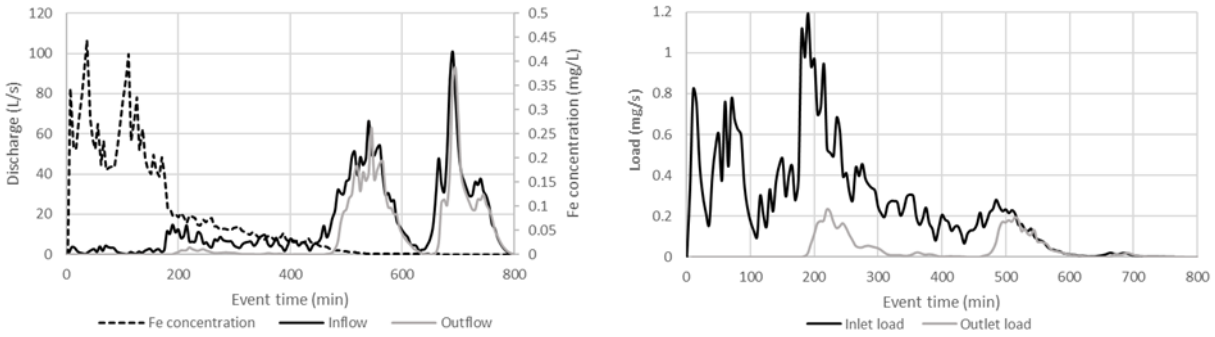

Figure 4.3: Events with the highest difference in quantity and Fe removal efficiencies.

Figure 4.4 shows the relation between quantitative and qualitative efficiency of the events for NO3 with higher w2 and TOC with lower w2. It can be observed that the removal efficiency of TOC is more linearly dependent on the quantitative efficiency, while nitrate has a greater variation. To illustrate this, two events with the greatest difference between quantitative and NO3 removal efficiencies were separated (Figure 4.5).

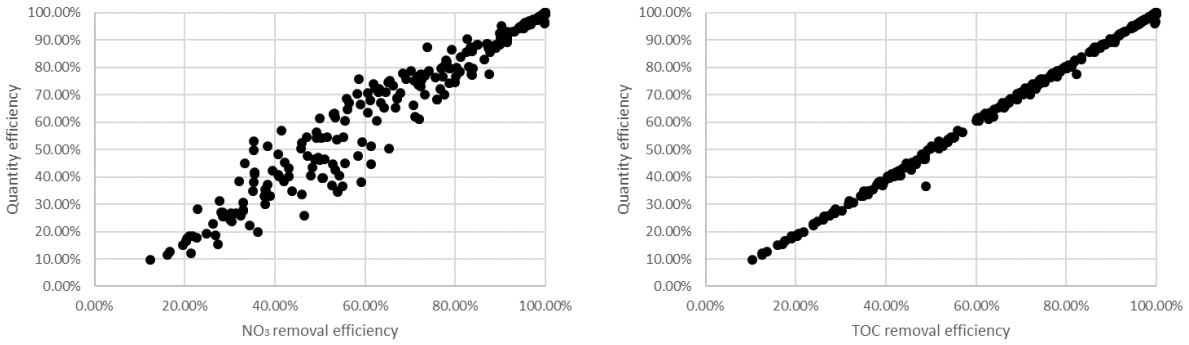

Figure 4.4: Influence of w2 on the relationship between quantitative and qualitative efficiency

For smaller values of w2, higher concentrations are found in lower flows. In Figure 4.5-a, the event with NO3 removal efficiency is lower than quantitative, the runoff portion with higher flow is absorbed at the beginning, when the water content in the soil layer is low and infiltration capacity is high. When the outflow begins, NO_3 concentration is high resulting in a higher mass output.

Figure 4.5-b shows the event with the highest removal efficiency. In this event, higher inflows surpass the bioretention capacity, when outflow with low NO_3 concentration occurs. When the outflow ceases with lower discharges, NO_3 concentration is much higher and most of its mass is retained.

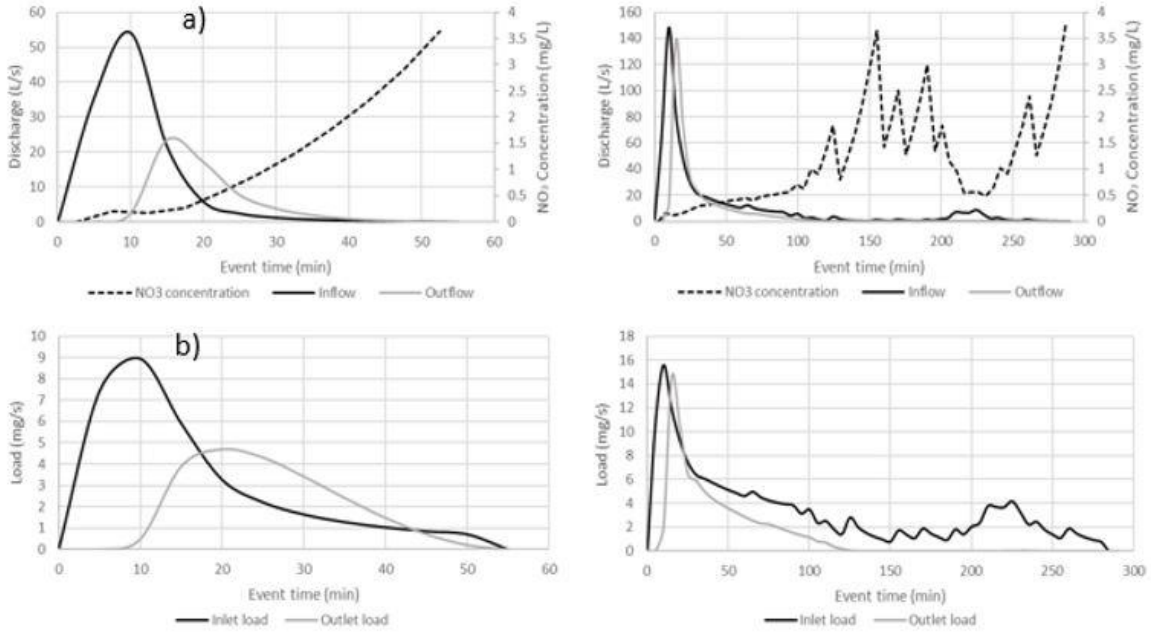

Figure 4.5: Examples of NO_3 removal

4.3.3.Rainfall desegregation and climate changes in Sao Carlos

Table 4.4 shows the disaggregation performance by the modified Bartlett-Lewis method. The number of wet cells, rainfall depth and the variance in each month present close values. The total disaggregated precipitation in the period was 4352.3mm, 2.8% greater than the observed. The number of wet cells in the disaggregated series was 6865, number 3.5% lower than that observed, of 7116. R^2 values between observed and simulated wet cells, ordered by the largest depths, were also satisfactory. The graphs showing this relationship, for each month, can be found in Appendix A15 and A16. Table 4.5 shows the difference of the total rainfall volume between the raw future scenarios and their disaggregated series. The largest difference can be observed from 1980 to 1999 with a 3% lower volume used in the simulations.

Table 4.4: Desegregated and observed rainfall

	Number of wet cells		Precipitation (mm)		Variance		
	Desegregated	**Observed**	**Desegregated**	**Observed**	**Desegregated**	**Observed**	**R^2**
Jan	1317	1420	810.69	815.80	0.038	0.041	0.959
Fev	725	714	565.43	539.00	0.056	0.052	0.979
Mar	916	858	562.89	530.40	0.034	0.029	0.968
Apr	259	240	135.90	129.40	0.0070	0.0064	0.988
May	684	713	375.48	351.60	0.016	0.013	0.949
Jun	366	344	209.20	192.20	0.011	0.011	0.951
Jul	206	192	89.24	82.60	0.0036	0.0036	0.957
Aug	37	35	16.01	17.00	0.00040	0.00059	0.958
Sep	420	448	245.93	240.60	0.014	0.012	0.987
Out	317	430	307.55	319.40	0.028	0.022	0.979
Nov	422	448	240.21	240.60	0.012	0.012	0.981
Dec	1196	1274	793.73	773.40	0.050	0.042	0.987
Total	6865	7116	4352.26	4232.00			

Table 4.5 shows the climate change impacts on temperature and precipitation in the city of São Carlos, as the data acquired from INPE suggest (Chou et al., 2014-a; Chou et al, 2014-b; Lyra et al, 2017).

Table 4.5: Climate changes impacts on temperature and precipitation

	1980-1999	**2020-2039**		**2040-2059**		**2060-2079**		**2080-2099**		**Difference in 1 century**	
		4.5	**8.5**	**4.5**	**8.5**	**4.5**	**8.5**	**4.5**	**8.5**	**4.5**	**8.5**
Average Temperature (ºC)	21.35	24.46	25.40	24.39	25.65	25.79	27.42	26.01	29.43	4.66	8.08
Total Precipitation (mm)	38926	23394	20093	27548	26649	23938	23061	23031	18771	-41%	-51%
Desegregation difference	-3.0%	2.6%	1.8%	-0.2%	-1.4%	-0.4%	-0.3%	-0.1%	0.3%	**Average**	**0.0%±0.2**

For the less optimistic scenario, RCP 8.5, an increase of approximately 8ºC in the average air temperature and a fall of almost 30% in the rainfall volume are expected. If the RCP scenario 4.5 occurs, it is estimated that the impacts will be milder, with an increase of almost 5ºC in the air temperature and a fall of 13% in the precipitation.

Table 4.6 shows the climate change impacts on the quantity and quality of runoff. The analysis was made disregarding the initial 6 months of warm-up for a better precision of the quality data.

Table 4.6: Estimated climate change impact on precipitation, runoff and pollutant washoff.

	1980-1999	2020-2039		2040-2059		2060-2079		2080-2099		Difference in 1 century	
		4.5	8.5	4.5	8.5	4.5	8.5	4.5	8.5	4.5	8.5
Runoff (mm)	7393.2	4296.5	3512.0	5267.9	4971.6	4551.3	4408.0	4153.4	3486.9	-43.8%	-52.8%
Fe (g/ha)	5425.1	5209.7	5060.8	5161.7	5216.6	4983.4	4964.3	5056.5	4948.7	-6.8%	-8.8%
NO3 (g/ha)	2473.3	2181.4	2015.8	2210.6	2187.2	2076.0	2032.0	2092.3	1911.1	-15.4%	-22.7%
NO2 (g/ha)	64.7	39.7	33.0	46.8	44.4	40.7	39.3	37.8	31.8	-41.6%	-50.8%
PO4 (g/ha)	172.9	152.6	141.6	154.5	156.6	144.0	145.0	148.0	140.2	-14.4%	-18.9%
TOC (g/ha)	14178.4	14271.7	13768.3	13891.7	14046.5	13687.7	13685.2	13858.0	13855.5	-2.3%	-2.3%
Zn (g/ha)	264.1	232.7	216.1	236.4	239.6	220.3	222.0	211.2	213.6	-20.0%	-19.1%

The input depth in the period between 1980 and 1999 is higher than all future periods for both scenarios, it falls to the 2020-2039 scenario, has an increment for the next period and continuously falls until 2080-2099. In 100 years, the drop in surface runoff is greater than the pollutant fall. The pollutant with the highest decrease was NO^2 with low coefficient w1, tending to follow the decrease in the inlet runoff volume. Fe with the highest w1 was the pollutant with the second lowest percentage drop. TOC, with lower exponent buildup, had a drop of only 2.3% in 100 years in both scenarios.

4.3.4.Climate change impacts on bioretention performance

Table 4.7 shows the outlet runoff depth and pollutant mass for each analyzed period for the two RCP scenarios.

Table 4.7: The climate change impacts on bioretention performance

	1980-1999	2020-2039		2040-2059		2060-2079		2080-2099	
		4.5	8.5	4.5	8.5	4.5	8.5	4.5	8.5
Runoff (mm)	1356.5	685.5	513.1	1079.3	1026.9	936.3	935.0	770.7	653.5
Quantity efficiency	81.7%	84.0%	85.4%	79.5%	79.3%	79.4%	78.8%	81.4%	81.3%
Fe	326.7	258.2	222.6	312.7	298.4	276.2	307.9	254.9	272.3
Fe removal	94.0%	95.0%	95.6%	93.9%	94.3%	94.5%	93.8%	95.0%	94.5%
NO3	202.7	147.4	125.7	179.9	176.9	166.3	173.7	155.4	153.7
NO3 removal	91.8%	93.2%	93.8%	91.9%	91.9%	92.0%	91.5%	92.6%	92.0%
NO2	9.8	5.1	3.9	7.7	7.4	6.7	6.7	5.6	4.9
NO2 removal	84.9%	87.0%	88.1%	83.5%	83.4%	83.4%	82.8%	85.2%	84.7%
PO4	21.6	16.4	14.4	19.6	19.9	17.7	19.7	17.1	16.7
PO4 removal	87.5%	89.3%	89.8%	87.3%	87.3%	87.7%	86.4%	88.4%	88.1%
TOC	1808.9	1514.3	1366.8	1732.5	1858.1	1716.2	1956.0	1715.1	1761.5
TOC removal	87.2%	89.4%	90.1%	87.5%	86.8%	87.5%	85.7%	87.6%	87.3%
Zn	34.03	25.57	22.49	30.84	31.78	27.95	31.46	25.20	26.33
Zn removal	87.1%	89.0%	89.6%	87.0%	86.7%	87.3%	85.8%	88.1%	87.7%

Despite the decrease in the runoff volume over the years, the quantity efficiency of bioretention tends to remain constant over the years. The efficiency for scenario 8.5 is a bit lower when compared to scenario 4.5, and is only higher in the near future between 2020 and 2039. The difference between efficiencies is more significant between periods than between scenarios. The periods between 2040 and 2079 show the lowest efficiencies in both scenarios, below 80%. The explanation is due to a higher percentage of stronger events.

The cells with a 3-hour timestep, which were subsequently disaggregated, were analyzed in Figure 4.6, showing the occurrence percentage of a given cell above a given depth.

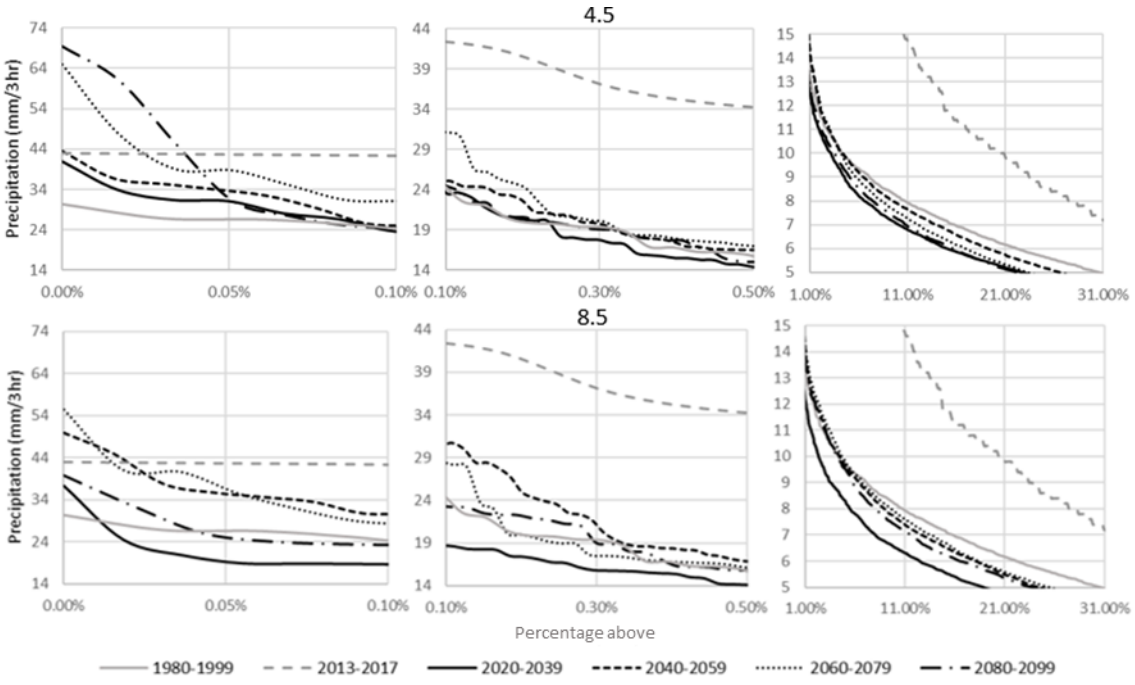

Figure 6: Rainfall regime over the years

It is observed that the periods 2040-2059 and 2060-2079 are generally more intense, explaining smaller quantitative efficiencies. The period from 2020 to 2039 presents the smallest depths, followed by the period from 2080 to 2099, periods with the highest efficiencies.

The periods 1980-1999 and 2013-2017 are in gray. For the older scenarios, it can be observed that the 0.5% more intense cells of these periods tend to be smaller than the other scenarios analyzed, only becoming greater between the 1% and 31% largest cells. The most recent period from 2013 to 2017 can be highlighted for events that are much higher than the other periods within the 1% and 31% largest events, which explains the much lower quantity and quality efficiencies. By analyzing rainfall events by the city intensity duration frequency curve (IDF), it can be observed that there were 17 rainfall events over 1 year of return time, suggesting a very atypical rainfall regime in the region during these years. An intense drought was also

recorded, which resulted in a water crisis in the region leading to rationing measures and economic losses in several sectors.

The pollutant removal efficiencies follow the trend of quantity efficiency, in which the periods 2040-2059 and 2060-2079 have lower removal percentages, as shown in Table 4.7. However, the removal efficiencies are greater than the quantity efficiency and, as observed between 2013 to 2017, the pollutants with higher washoff coefficient w1 are the ones with the highest removal efficiency. Fe generally presents greater efficiency for the scenarios, above 93%, while NO2 presents the lowest percentage retained, at most 88.1%.

Despite the decrease in the pollutant mass washed in 100 years, the EMC increases as shown in Table 4.8. The concentration of TOC is the most affected by climate change, while NO2 has the lowest growth.

TOC has the lowest buildup recovery rate of b2, and with more frequent rainfall events from 1980 to 1999, it becomes harder to recover its maximum buildup. With climate changes, however, longer dry times allow this pollutant to reach higher buildup, also explaining the lower mass drop of this pollutant in 100 years.

Table 4.8 also shows that bioretention is able to soften the EMC growth. The bioretention efficiency is greater in the initial moments of the event, with drier surface soil and when the first flush occurs. Thus, this phenomenon with higher concentrations, is absorbed more easily, while the cleaner runoff tends to leave the bioretention more frequently. This reduction is also influenced by parameter w1. Fe (highest w1) had the largest EMC reduction while NO2 had the lowest. TOC, despite the highest EMC increase, presented the second smallest EMC reduction. This pollutant buildup reaches higher levels in future scenarios, but its fall is slower due to a low

w1. It results in a greater constancy in concentration, which decreases the bioretention capacity in reducing EMC levels.

Table 4.8: Climate change impacts on EMC and its reduction by the bioretention.

	4.5											
	Fe		**NO3**		**NO2**		**PO4**		**TOC**		**Zn**	
	EMC in	**EMC out**	**EMC in**	**EMC out**	**EMC in**	**EMC out**	**EMC in**	**EMC out**	**EMC in**	**EMC out**	**EMC in**	**EMC out**
1980-1999	0.7	0.24	0.33	0.15	0.0088	0.0072	0.023	0.016	1.92	1.3	0.036	0.025
2020-2039	1.21	0.38	0.51	0.22	0.0092	0.0075	0.036	0.024	3.32	2.2	0.054	0.037
2040-2059	0.98	0.29	0.42	0.17	0.0089	0.0072	0.029	0.018	2.64	1.6	0.045	0.029
2060-2079	1.1	0.29	0.46	0.18	0.0089	0.0072	0.032	0.019	3.01	1.8	0.048	0.030
2080-2099	1.22	0.33	0.50	0.20	0.0091	0.0073	0.036	0.022	3.34	2.2	0.051	0.033
Difference in 100 years	65.91%	37.31%	50.58%	34.92%	3.95%	0.75%	52.35%	39.60%	73.98%	66.88%	42.35%	30.31%
Average EMC reduction	70.5% (±2.3)		58.9%(±2.1)		19.1%(±0.85)		36.1%(±3.2)		35.1%(±3.4)		34.3%(±3.3)	
	8.5											
	Fe		**NO3**		**NO2**		**PO4**		**TOC**		**Zn**	
	EMC in	**EMC out**	**EMC in**	**EMC out**	**EMC in**	**EMC out**	**EMC in**	**EMC out**	**EMC in**	**EMC out**	**EMC in**	**EMC out**
1980-1999	0.73	0.24	0.33	0.15	0.0088	0.0072	0.023	0.016	1.9	1.33	0.036	0.025
2020-2039	1.2	0.32	0.47	0.18	0.0077	0.0057	0.033	0.021	3.2	1.99	0.050	0.033
2040-2059	1.0	0.28	0.42	0.16	0.0084	0.0068	0.030	0.018	2.7	1.72	0.045	0.029
2060-2079	1.1	0.33	0.45	0.19	0.0086	0.0072	0.032	0.021	3.0	2.09	0.049	0.034
2080-2099	1.2	0.35	0.46	0.20	0.0091	0.0075	0.034	0.022	3.3	2.29	0.051	0.034
Difference in 100 years	62.37%	46.73%	37.54%	33.49%	3.41%	4.10%	44.41%	36.48%	73.95%	71.40%	43.96%	36.17%
Average EMC reduction	70.4%(±1.9)		58.4%(±2.2)		19.2%(±3.26)		35.1%(±2.1)		33.1%(±3.0)		32.9%(±2.1)	

4.4.Conclusions

Using a specific model, this study verified the performance of a bioretention located in a subtropical climate. It analyzed the quantity efficiency, the relation between the peak flow and its reduction, and the removal efficiency of Fe, NO3, NO2, PO4, TOC and Zn separately according to their washoff/buildup parameters.

The climate change impacts were also estimated in the city of São Carlos for RCP 4.5 and 8.5. Both scenarios point to a reduction in rainfall volume in the city by 13% and 29%

respectively. However, the mass of the pollutants washed varies according to their specific washing characteristic.

However, climate change does not affect quantity efficiency, and therefore bioretention continues to contribute in retaining runoff volume. The results also show that the bioretention, even considering only the outflow without the treatment within its filtering media, contributes to reducing the pollutant concentration. The results of this paper show that LIDs can be incorporated into traditional drainage systems to mitigate not only the impacts of urbanization but also from climate changes.

Only the effects of climate change on LID performance were analyzed in this study. However, the bioretention is located in an area where urbanization is expected to grow, from approximately 20% today to 80% in 2100 (Rosa, 2016). Therefore, it is recommended to assess the climate change and urbanization impacts combined in the catchment to more accurately verify the bioretention performance by the end of the century.

4.5. References

Back, Á. J., Uggioni, E., & Vieira, H. J. (2011). Modeling precipitation of short duration by means of the modified Bartlett-Lewis rectangular pulse model. *Revista Brasileira de Meteorologia*, *26*(3), 461-472.

Chou, S. C., Lyra, A., Mourão, C., Dereczynski, C., Pilotto, I., Gomes, J., ... & Campos, D. (2014). Evaluation of the Eta simulations nested in three global climate models. *American Journal of Climate Change*, *3*(5), 438-454.

Chou, S. C., Lyra, A., Mourão, C., Dereczynski, C., Pilotto, I., Gomes, J., ... & Campos, D. (2014). Assessment of climate change over South America under RCP 4.5 and 8.5 downscaling scenarios. *American Journal of Climate Change*, *3*(5), 512-525.

De Dios, V. R., Roy, J., Ferrio, J. P., Alday, J. G., Landais, D., Milcu, A., & Gessler, A. (2015). Processes driving nocturnal transpiration and implications for estimating land evapotranspiration. *Scientific reports*, *5*, srep10975.

EMBRAPA - Empresa Brasileira de Pesquisa Agropecuária/Embrapa Pecuária Sudeste, 2016. Condições meteorológicas da estação da Embrapa Pecuária Sudeste. 〈 http://www.cppse.embrapa.br/meteorologia/index.php?pg=inicio (Accessed 12/08/2017)

Fletcher, T. D., Andrieu, H., & Hamel, P., 2013. Understanding, management and modelling of urban hydrology and its consequences for receiving waters: A state of the art. Advances in Water Resources, 51, 261-279.

Guan, M., Sillanpää, N., & Koivusalo, H., 2015. Modelling and assessment of hydrological changes in a developing urban catchment. Hydrological Processes, 29(13), 2880-2894.

Green, W.H.; Ampt, G. A.(1911) - Studies on soil physics-Part I-The flow of air and water through soils. J of Agric. Sci IV, May:1-24

Hunt, W. F., Smith, J. T., Jadlocki, S. J., Hathaway, J. M., & Eubanks, P. R. (2008). Pollutant removal and peak flow mitigation by a bioretention cell in urban Charlotte, NC. *Journal of Environmental Engineering*, *134*(5), 403-408.

INSTITUTO BRASILEIRO DE GEOGRAFIA E ESTATÍSTICA (2016). *Pesquisa Nacional por Amostra de Domicílios*. Rio de Janeiro.

Lucas, W. C., & Sample, D. J. (2015). Reducing combined sewer overflows by using outlet controls for Green Stormwater Infrastructure: Case study in Richmond, Virginia. *Journal of Hydrology*, 520, 473–488. http://doi.org/10.1016/j.jhydrol.2014.10.029

Lyra, A., Tavares, P., Chou, S. C., Sueiro, G., Dereczynski, C., Sondermann, M., ... & Giarolla, A. (2016). Climate change projections over three metropolitan regions in Southeast Brazil

using the non-hydrostatic Eta regional climate model at 5-km resolution. *Theoretical and Applied Climatology*, 1-20.

Macedo, M. B. D., Lago, C. A. F. D., Mendiondo, E. M., & Souza, V. C. B. D. (2018). Performance of bioretention experimental devices: contrasting laboratory and field scales through controlled experiments. *RBRH*, *23*.

Macedo, M. B., Rosa, A., do Lago, C. A. F., Mendiondo, E. M., & de Souza, V. C. B., 2017. Learning from the operation, pathology and maintenance of a bioretention system to optimize urban drainage practices. Journal of Environmental Management, 204, 454-466.

Malek, E. (1992). Night-time evapotranspiration vs. daytime and 24h evapotranspiration. *Journal of hydrology*, *138*(1-2), 119-129.

Marengo, J. & Ambrizzi, T. (2014) Instituto Nacional de Ciência e Tecnologia de Mudanças Climáticas II. *Processo CNPq 465501/2014-1*, INCT-MC-II (FAPESP 2014/50848-9).

Miranda, M. D., Pinto, H., Júnior, J., Fagundes, R., Fonsechi, D., Calve, L., & PELLEGRINO, G. (2009). A classificação climática de Koeppen para o estado de São Paulo. *CEPAGRI-Centro de Pesquisas Meteorológicas e Climáticas Aplicadas à Agricultura. CPA-UNICAMP. Campinas-SP*.

Piro, P., & Carbone, M. (2014). A modelling approach to assessing variations of total suspended solids (TSS) mass fluxes during storm events. *Hydrological Processes*, *28*(4), 2419-2426.

Rodriguez-Iturbe, I., & Isham, V. (1987, April). Some models for rainfall based on stochastic point processes. In *Proc. R. Soc. Lond. A* (Vol. 410, No. 1839, pp. 269-288). The Royal Society.

Porto, R. M. (2006) Hidráulica básica. 4. ed. São Carlos: São Carlos School of Engineering-Universidade de Sao Paulo.

Rodriguez-Iturbe, I., & Isham, V. (1988, June). A point process model for rainfall: further developments. In *Proc. R. Soc. Lond. A* (Vol. 417, No. 1853, pp. 283-298). The Royal Society.

Rossman, L. A. (2010). *Storm water management model user's manual, version 5.0* (p. 276). Cincinnati: National Risk Management Research Laboratory, Office of Research and Development, US Environmental Protection Agency.

Rosa, A. (2016). *Bioretention for diffuse pollution control in TC using experimental-adaptative approaches of ecohydrology* . PhD Thesis. School Of Engineering At São Carlos, University Of São Paulo, São Carlos, Brazil.

Sillanpää, N., & Koivusalo, H., 2015. Stormwater quality during residential construction activities: influential variables. Hydrological Processes, 29(19), 4238-4251.

Soil Science Division Staff., 2017. Soil survey manual. C. Ditzler, K. Scheffe, and H.C. Monger (eds.). USDA Handbook 18. Government Printing Office, Washington, D.C

Sun, S., Barraud, S., Branger, F., Braud, I., & Castebrunet, H., 2017. Urban hydrologic trend analysis based on rainfall and runoff data analysis and conceptual model calibration. Hydrological Processes, 31(6), 1349-1359.

Sun, Y., Tong, S., & Yang, Y. J., 2016. Modeling the cost-effectiveness of stormwater best management practices in an urban watershed in Las Vegas Valley. Applied Geography, 76, 49-61.

Van Vuuren, D. P., Edmonds, J., Kainuma, M., Riahi, K., Thomson, A., Hibbard, K., ... & Masui, T., 2011. The representative concentration pathways: an overview. *Climatic change*, *109*(1-2), 5.

5.GENERAL CONCLUSIONS

In Chapter 3, the runoff quantity and quality were characterized. In this chapter, a sensitivity analysis clarified how the buildup and washoff parameters influence the predicted inputs of pollutants. This Chapter also presented the washoff exponential equation chosen in the simulations and the correct warm-up period. Concerning the results in this chapter, the quality load-based calibration presented a greater proximity of the total mass and the EMC, between predicted and observed loads, even with a higher difference in the mean concentrations. This Chapter also seasonally estimated the runoff quality draining into an existing LID/bioretention technique. These seasons corresponded to drier periods ("subtropical winter"), wetter ("subtropical summer"), post-wet ("subtropical fall") and post-dry ("subtropical spring") periods. Therefore, the results in Chapter 3 help to achieve the first specific objective. "*Characterize the urban runoff in a subtropical catchment, in terms of volume, flow and water quality, elucidating the runoff generation and pollutants wash-off processing, using a stepwise flowchart including calibration, validation and sensitivity analysis*.".

The specific purpose 2 "*Analyze the impacts of climate changes on a subtropical urban drainage."* was investigated in Chapter 3. The RCP 4.5 and 8.5 for four future periods were compared to the current one. The results compared the temperature, total rainfall volumes, rainfall intensity, runoff volume, total pollutants mass and EMC. For both scenarios, the average temperature tends to increase while rainfall and runoff volumes decrease. Pollutant mass tends to decrease less then runoff, while the concentration increases. The variation of pollutant concentration throughout the scenarios depends on each buildup/washoff parameter, as was investigated in the first specific objective.

The general purpose "*To elucidate how runoff generation and pollutant wash-off processes respond to upstream factors of an experimental LID technique and, evaluate how this practice would perform as a local adaptation strategy considering rainfall-runoff scenarios under climate change.*' was also investigated in Chapter 3 and could be reached after the specific purposes. Quantity efficiency slightly varies around 80% over the years for both scenarios and climate change seems to have little impact on it. However, quality efficiency and EMC reduction varies from pollutants according to their buildup/washoff parameters and the possible reasons could be explained after investigating the specific purposes in Chapters 3 and 4. Besides the fact that quantity efficiency has been maintained, the EMC reduction tends to be improved with climate changes. These results showed that the hypothesis" *(...) decreasing stormwater retention and pollutant removal performance of LID practices*" was not confirmed.

Recommendations for future research

1- Quality simulations using buildup/washoff were studied in this dissertation, however NH_3, Cd and COD could not be validated suggesting that this model was not satisfactory for these pollutants. Therefore, other quality models have to be investigated in a subtropical climate to verify which one better represents the hydrological processes involved in this climate.

2- A single bioretention performance was analyzed in the microdrainage. Further studies are required to better evaluate the climate change impacts on the sustainable urban drainage, which comprises several units and types of LIDs.

3- The quality efficiency was obtained not considering physical processes on the bioretention surface. It is recommended to characterize the pollutant concentration on sediments per granulometric size, thus addressing the sedimentation process.

4- In addition, it was supposed that no chemical reaction occurred inside the bioretention, during the simulations. For a better precision in quality efficiency, these reactions need to be studied and eventually included in the mass balance.

5- Third generation LIDs, which aim to reuse water and nutrients, are currently being studied. This dissertation showed that climate change will alter the quantity of runoff and pollutants, and will possibly affect the resource reuse. Therefore, these impacts on third generation LIDs can also be measured.

6- The studied area is currently under occupation, altering the runoff quantity and quality. Then, land use and climate change combined impacts need to be quantified.

APPENDIX

A1- Sensitive analysis of the maximum buildup. In this case, w1=0.5, w2=1 and b2=0.02 $days^{-1}$.

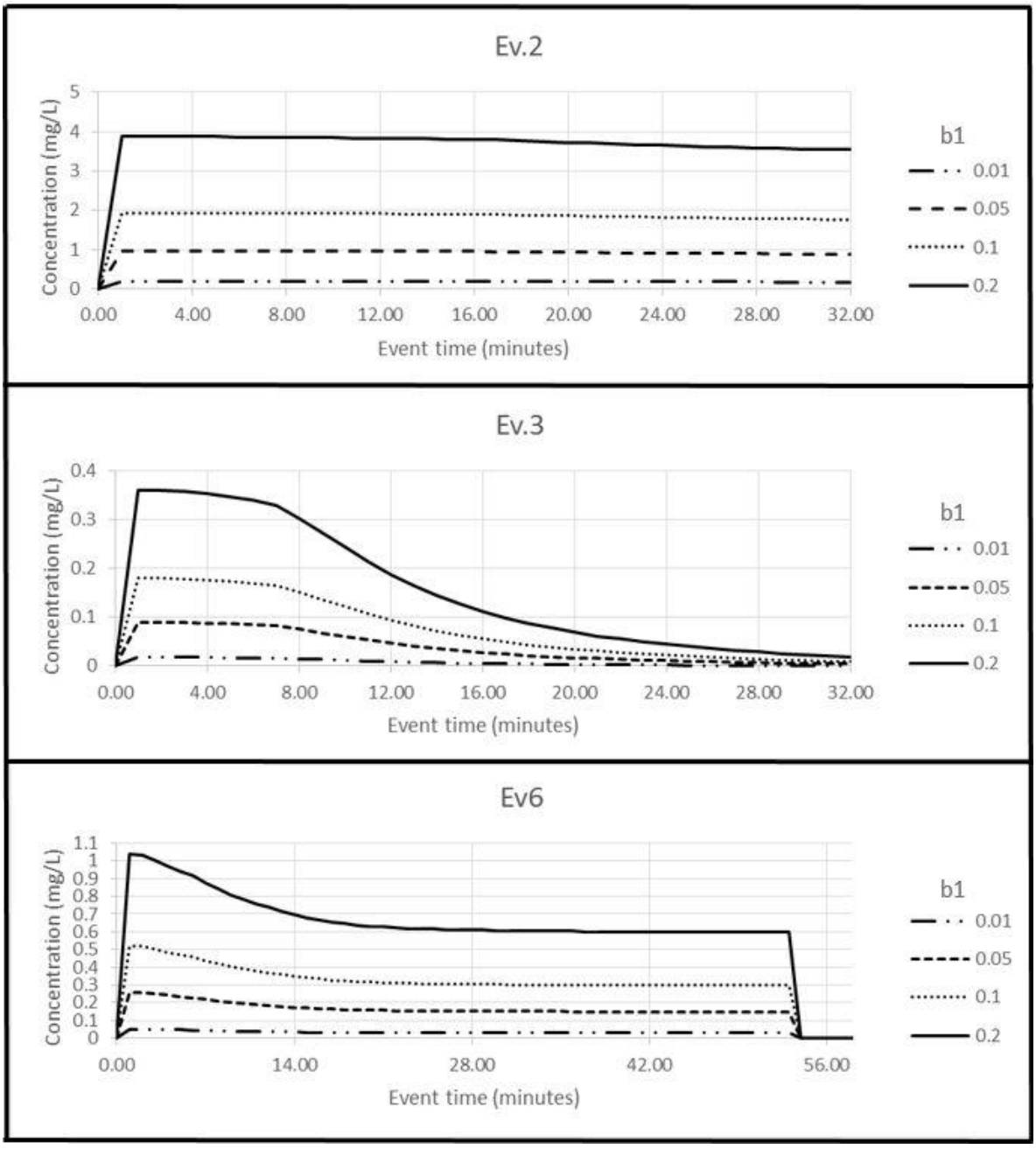

A2- Sensitive analysis of the washoff for w2 =1. In this case, b1=0.1 kg/ha and b2=0.02 $days^{-1}$.

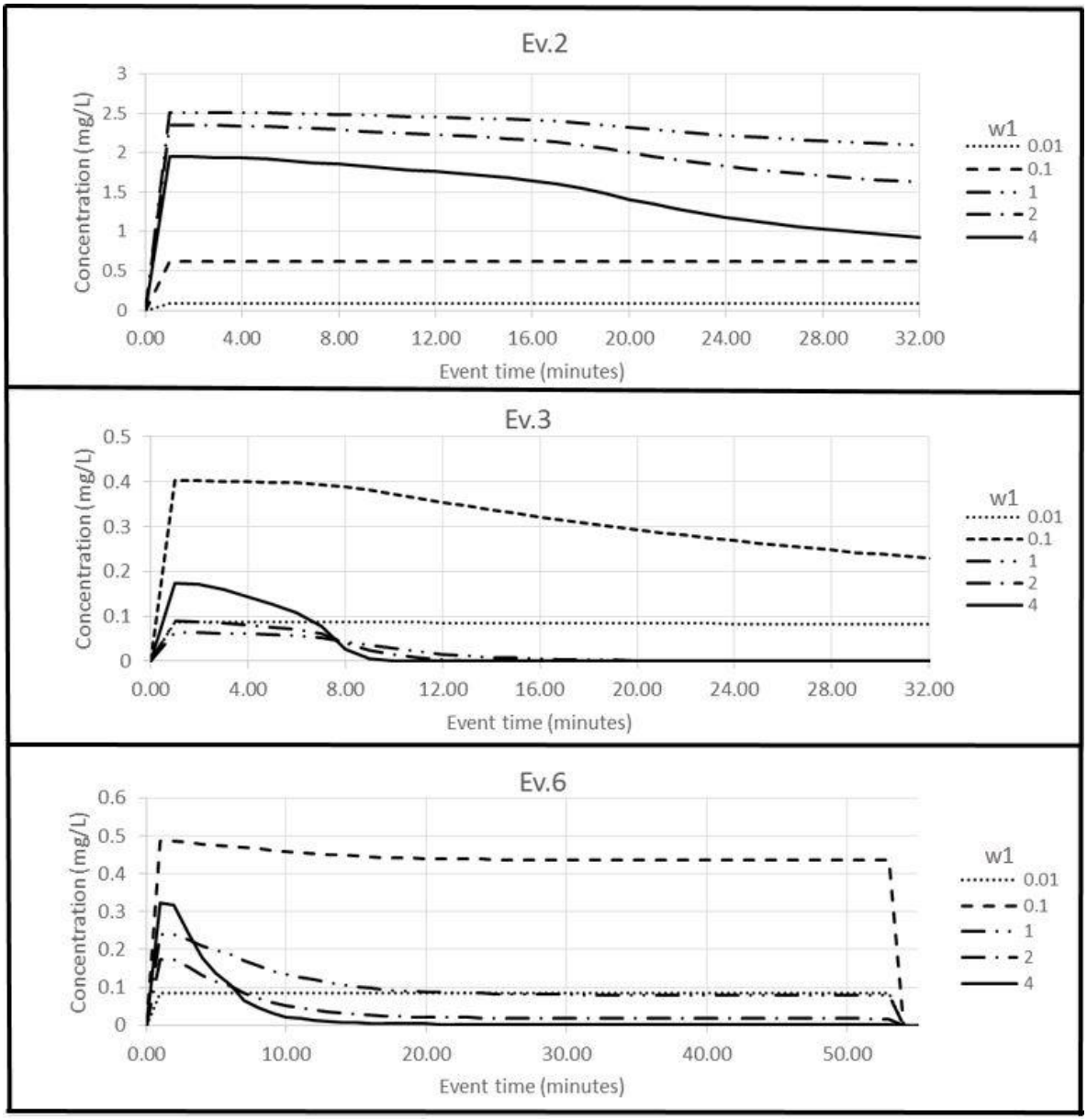

A3- Pollutograph and load calibration evaluation with NSE and VE and R^2.

		Concentration-based Calibration						Load-based Calibration					
		Concentration curve			Load curve			Concentration curve			Load curve		
		VE	NSE	R^2	VE	NSE	R^2	VE	NSE	R^2	VE	NSE	R^2
Cd	Ev.2	0.75	-21.27	0.00	0.84	0.87	0.97	0.71	-24.18	0.01	0.87	0.95	0.97
	Ev.3	0.79	-52.47	0.69	0.87	0.89	0.97	0.80	-61.35	0.71	0.91	0.96	0.98
	Ev.6	-4.39	-131.21	0.16	-6.18	-54.83	0.93	-3.80	-104.23	0.16	-5.41	-43.23	0.93
COD	Ev.2	0.57	-0.46	0.48	0.45	-1.67	0.68	-0.09	-28.57	0.41	0.76	0.65	0.75
	Ev.3	0.70	0.53	0.59	0.60	0.41	0.42	0.68	0.46	0.64	0.62	0.40	0.49
	Ev.6	-0.93	-3.42	0.01	-0.41	-0.56	0.24	-1.70	-8.72	0.01	-0.31	0.12	0.28
Fe	Ev.2	0.79	0.72	0.72	0.69	0.32	0.84	-0.18	-33.55	0.63	0.88	0.85	0.91
	Ev.3	-1.11	-90.62	0.22	0.04	-3.03	0.40	-0.34	-55.73	0.12	0.64	0.62	0.62
	Ev.6	-1.41	-4.14	0.34	-0.45	-1.36	0.97	-1.45	-6.17	0.01	0.48	0.84	0.95
NH4	Ev.2	0.74	0.33	0.44	0.64	0.00	0.86	0.48	-7.77	0.37	0.85	0.84	0.90
	Ev.3	0.90	0.70	0.71	0.93	0.97	0.98	0.74	-0.72	0.34	0.82	0.79	0.88
	Ev.6	-0.65	-170.97	0.07	-0.06	-0.16	0.98	-1.07	-335.66	0.10	0.37	0.70	0.95
NO3	Ev.2	0.57	0.18	0.42	0.26	-4.85	0.51	-6.89	-1658.66	0.28	0.80	0.69	0.78
	Ev.3	0.79	0.83	0.88	0.76	0.59	0.97	0.16	-7.44	0.92	0.81	0.80	0.83
	Ev.6	0.61	-0.43	0.23	0.62	0.78	0.92	-1.11	-59.32	0.00	0.45	0.58	0.80
NO2	Ev.2	0.81	0.44	0.51	0.79	0.75	0.89	0.73	-0.12	0.47	0.84	0.84	0.91
	Ev.3	0.91	0.87	0.92	0.91	0.97	0.97	0.92	0.88	0.89	0.90	0.95	0.95
	Ev.6	0.84	-0.71	0.00	0.76	0.89	0.97	0.68	-3.41	0.00	0.80	0.93	0.97
TOC	Ev.2	0.82	0.40	0.47	0.84	0.88	0.95	0.82	0.28	0.47	0.87	0.91	0.95
	Ev.3	0.87	0.69	0.93	0.93	0.95	0.97	0.86	0.67	0.93	0.92	0.96	0.97
	Ev.6	0.16	-0.04	0.01	0.60	0.82	0.87	0.18	-0.04	0.01	0.65	0.85	0.87
PO4	Ev.2	0.91	-0.47	0.08	0.87	0.88	0.98	0.84	-2.31	0.06	0.89	0.96	0.97
	Ev.3	0.76	0.30	0.36	0.77	0.69	0.95	0.75	-0.28	0.15	0.89	0.90	0.93
	Ev.6	0.83	-0.29	0.34	0.84	0.96	0.98	0.84	-0.31	0.23	0.89	0.98	0.98
Zn	Ev.2	0.91	-1.17	0.63	0.97	0.99	1.00	0.88	-3.39	0.59	0.95	0.99	1.00
	Ev.3	0.94	0.42	0.82	0.93	0.96	0.98	0.94	0.54	0.76	0.94	0.97	0.98
	Ev.6	0.69	0.10	0.60	0.71	0.88	0.94	0.72	0.25	0.56	0.71	0.88	0.94

A4- Ammonia calibration and validation

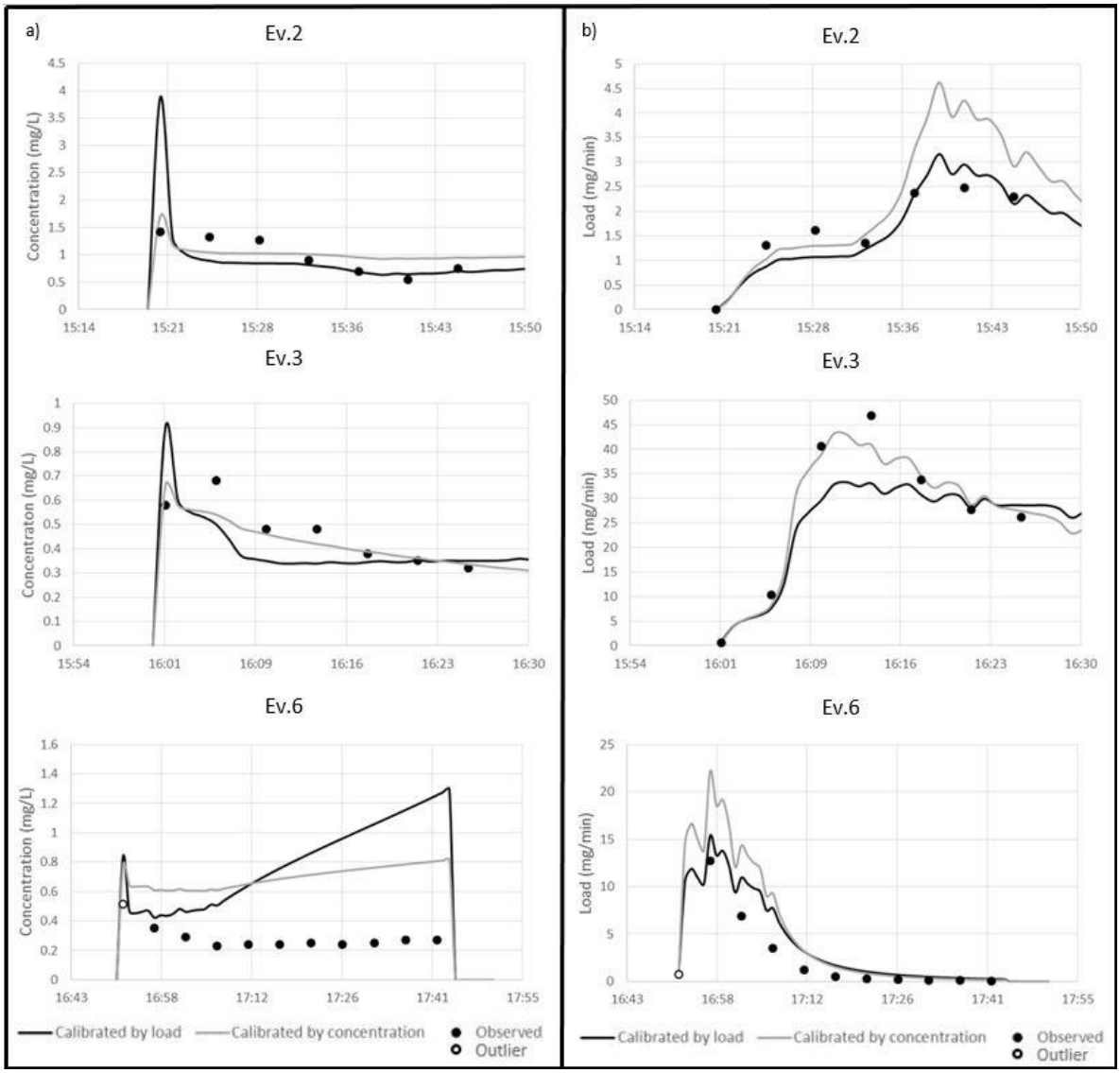

A5 – Cd calibration and validation

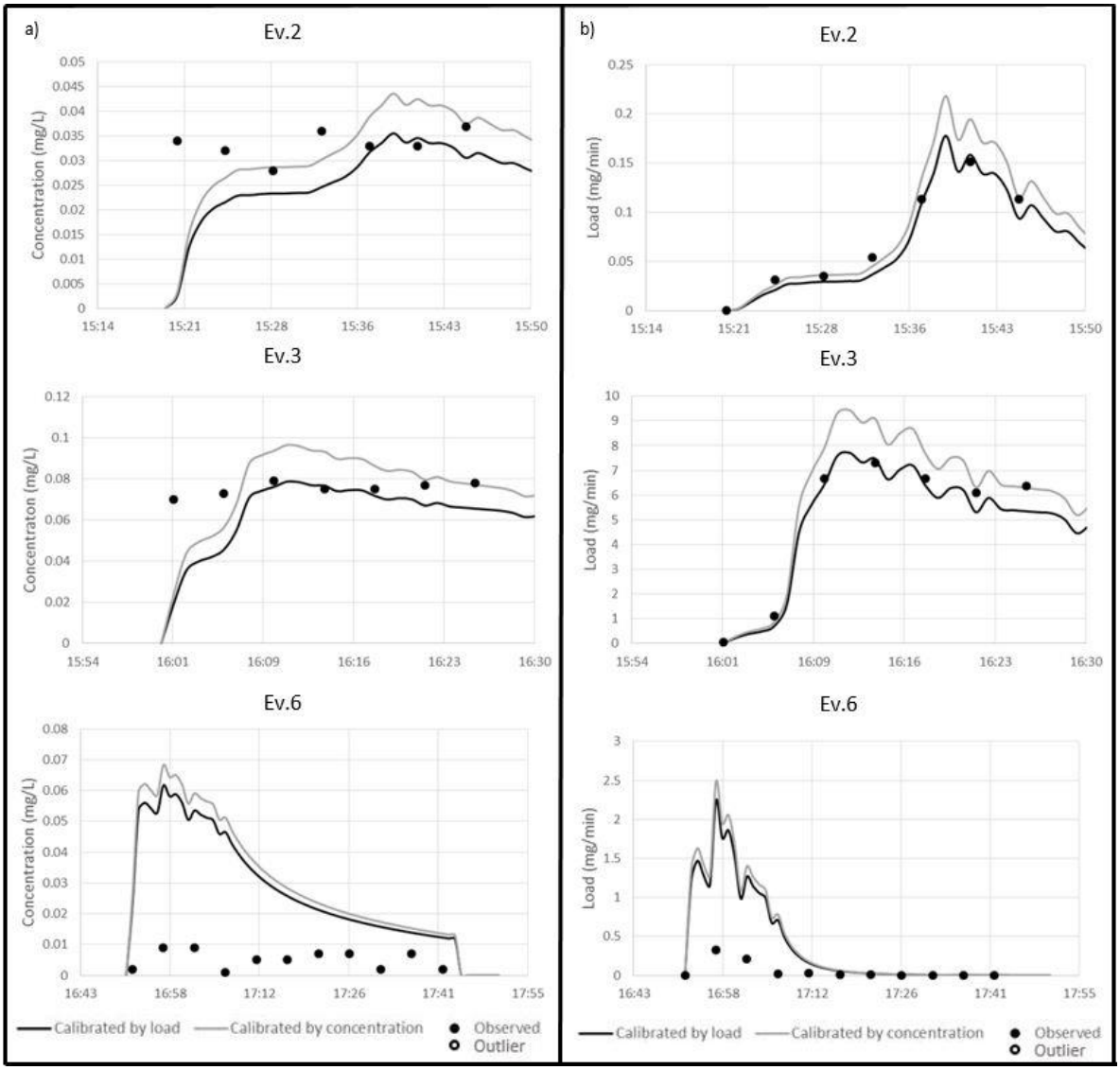

A6 – COD calibration and validation

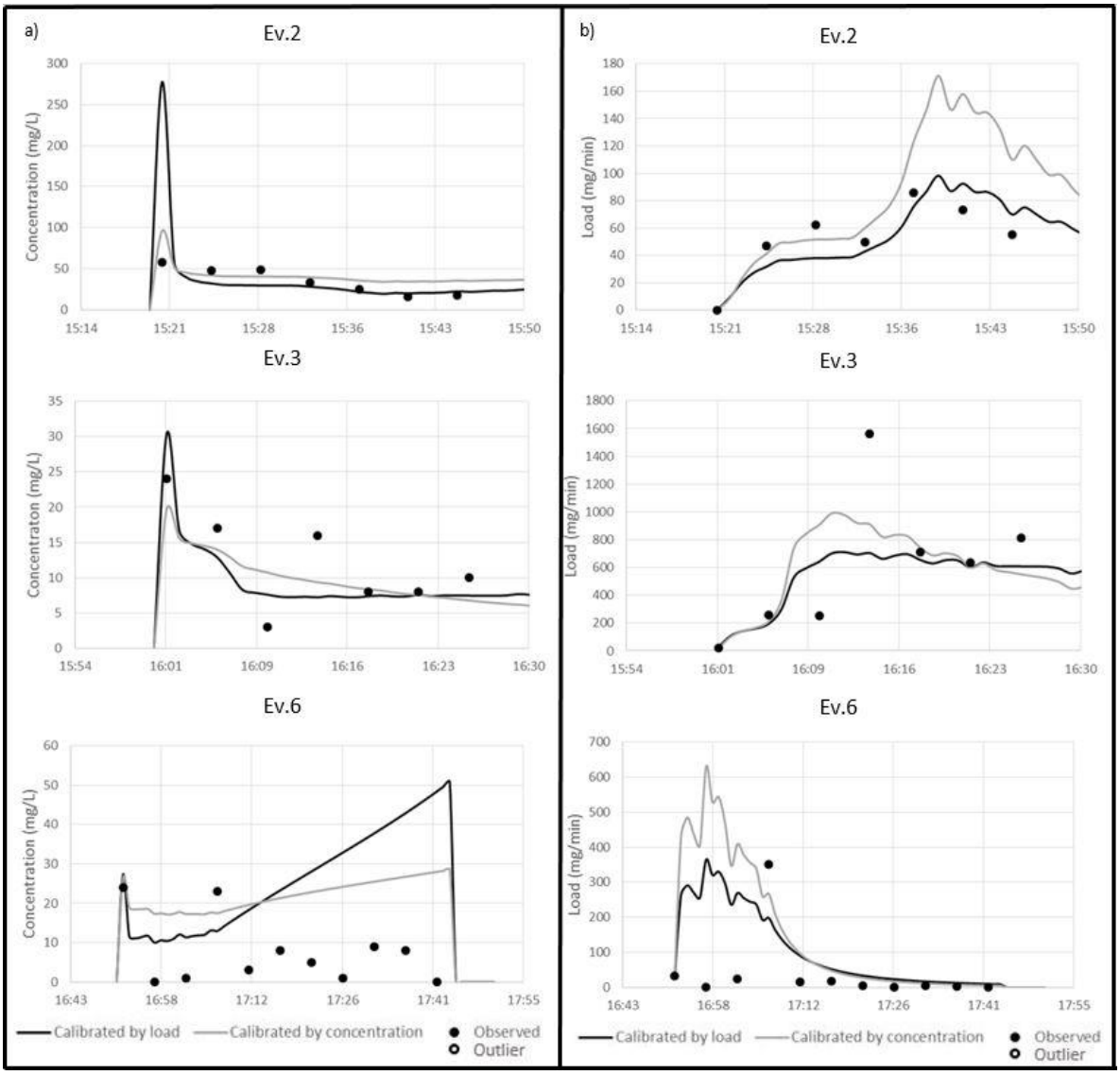

A7 – Fe calibration and validation

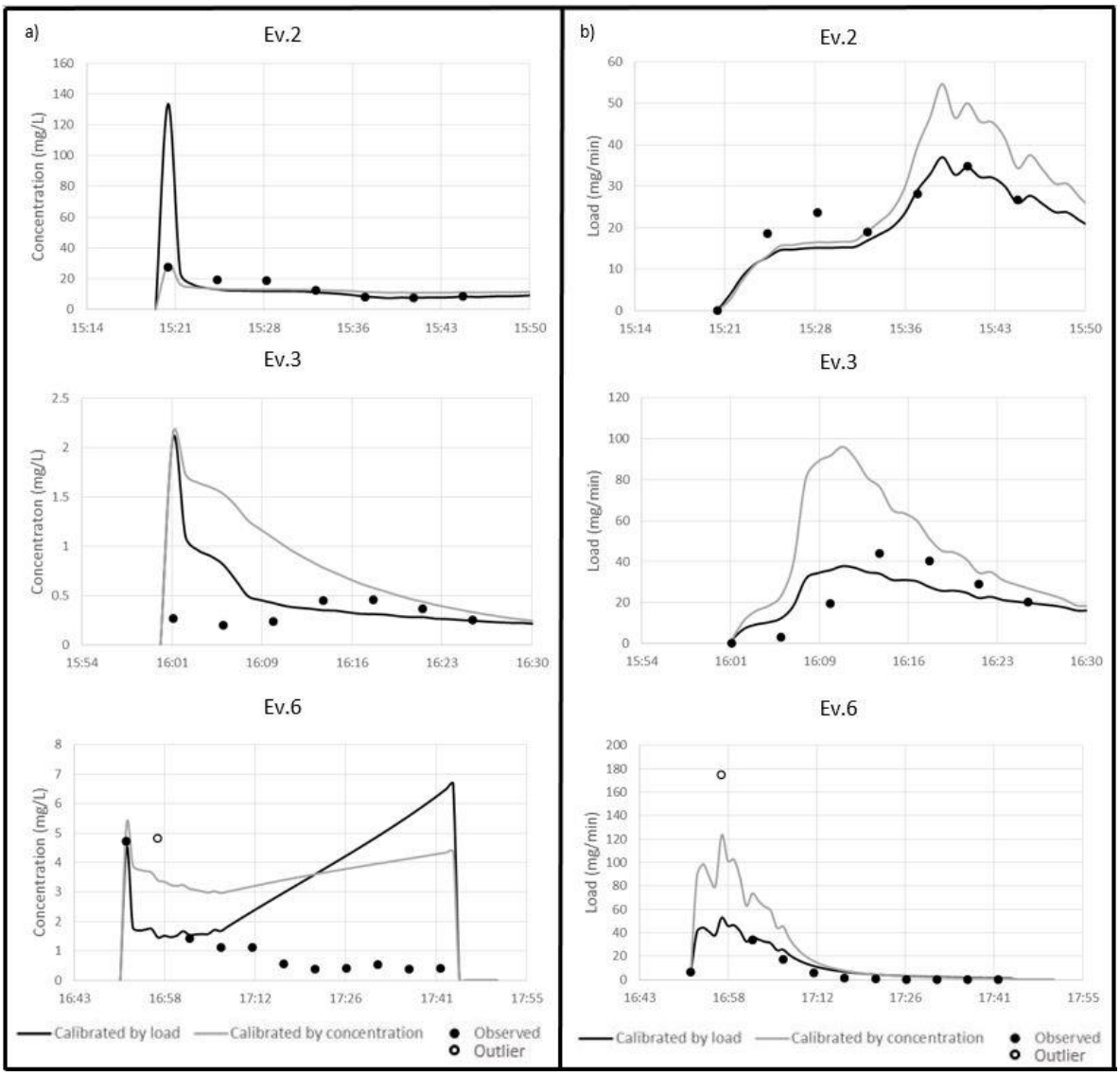

A8 – Nitrate calibration and validation

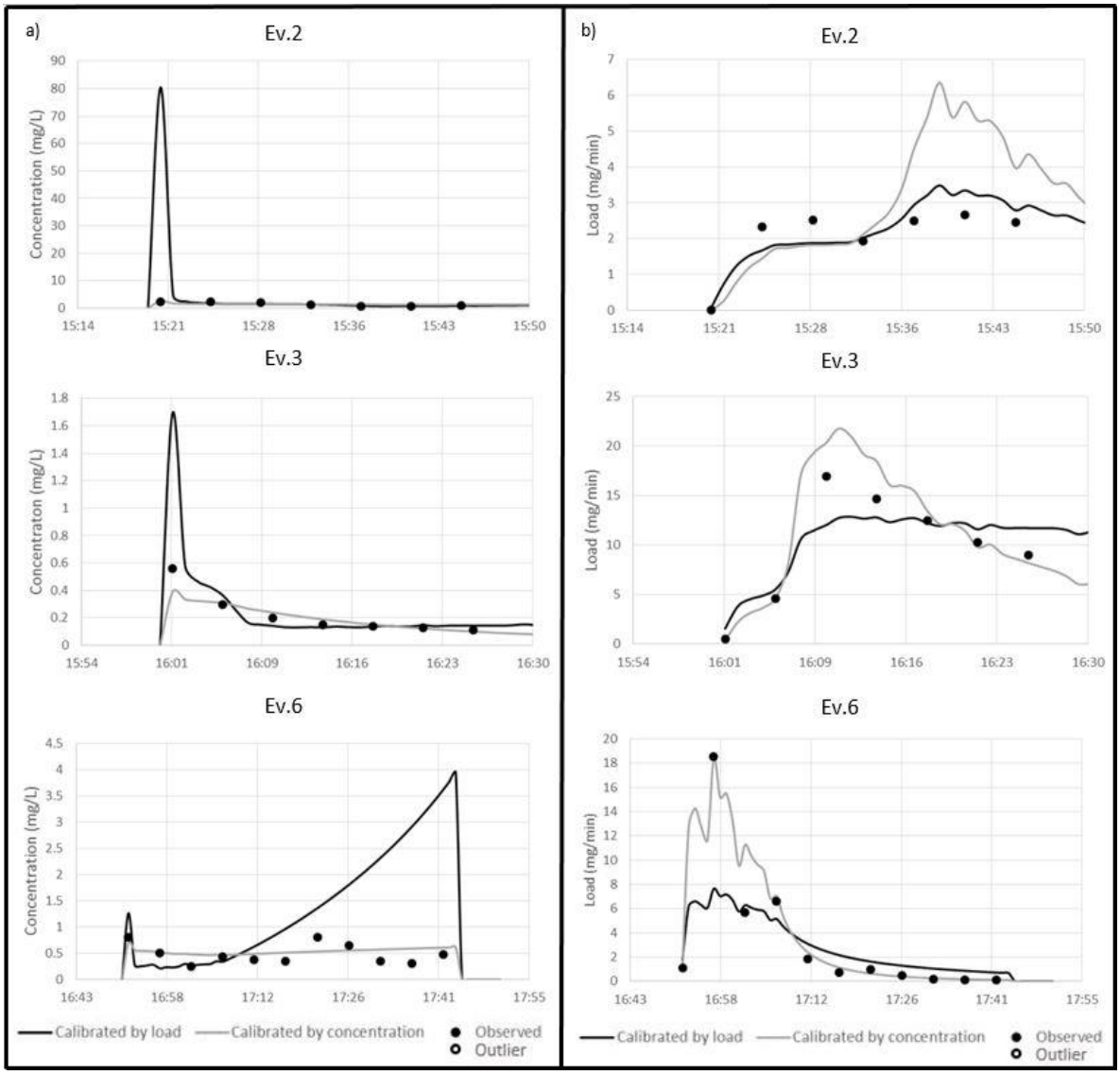

A9 – Nitrite calibration and validation

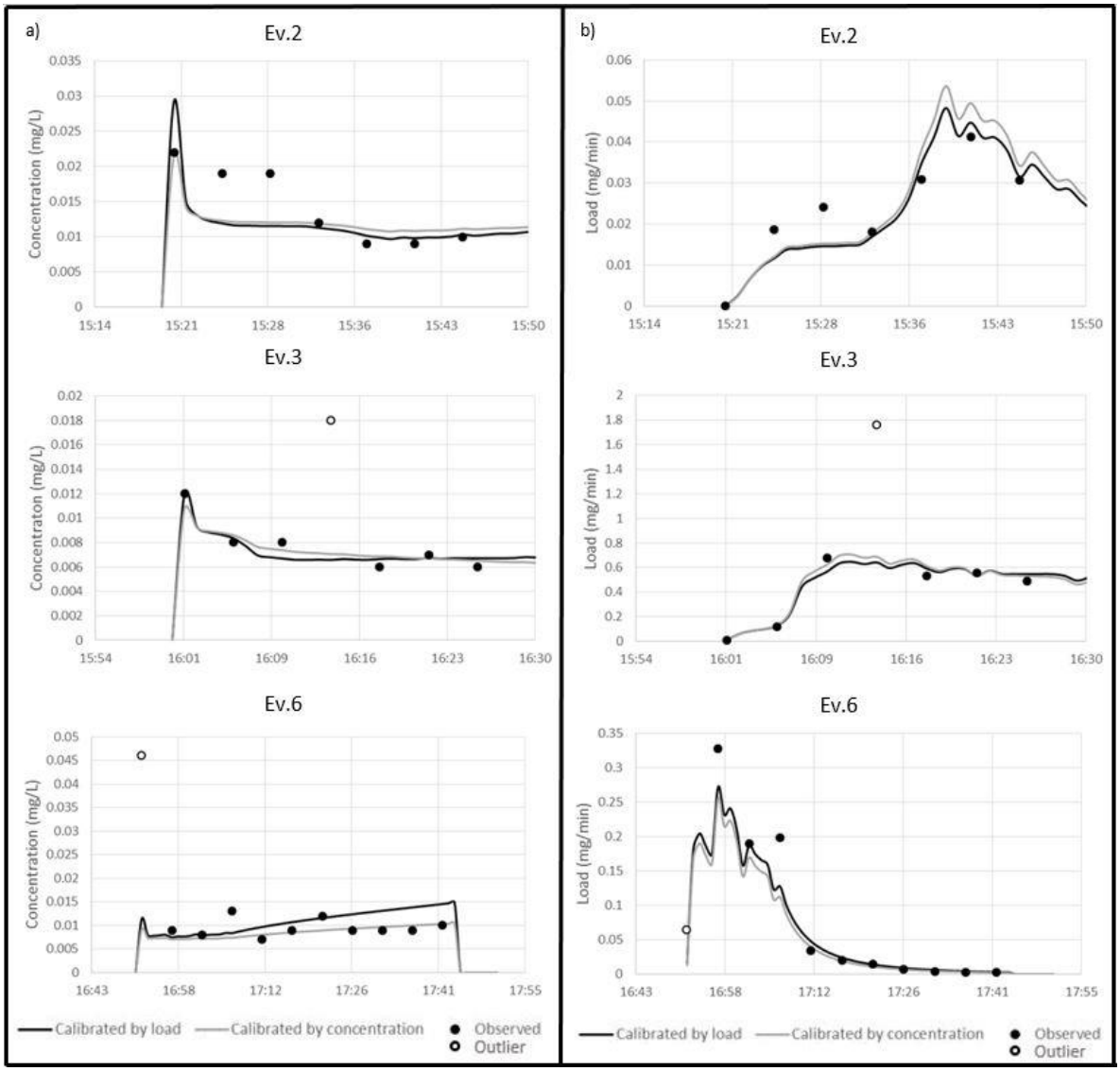

A10 – Phosphate calibration and validation

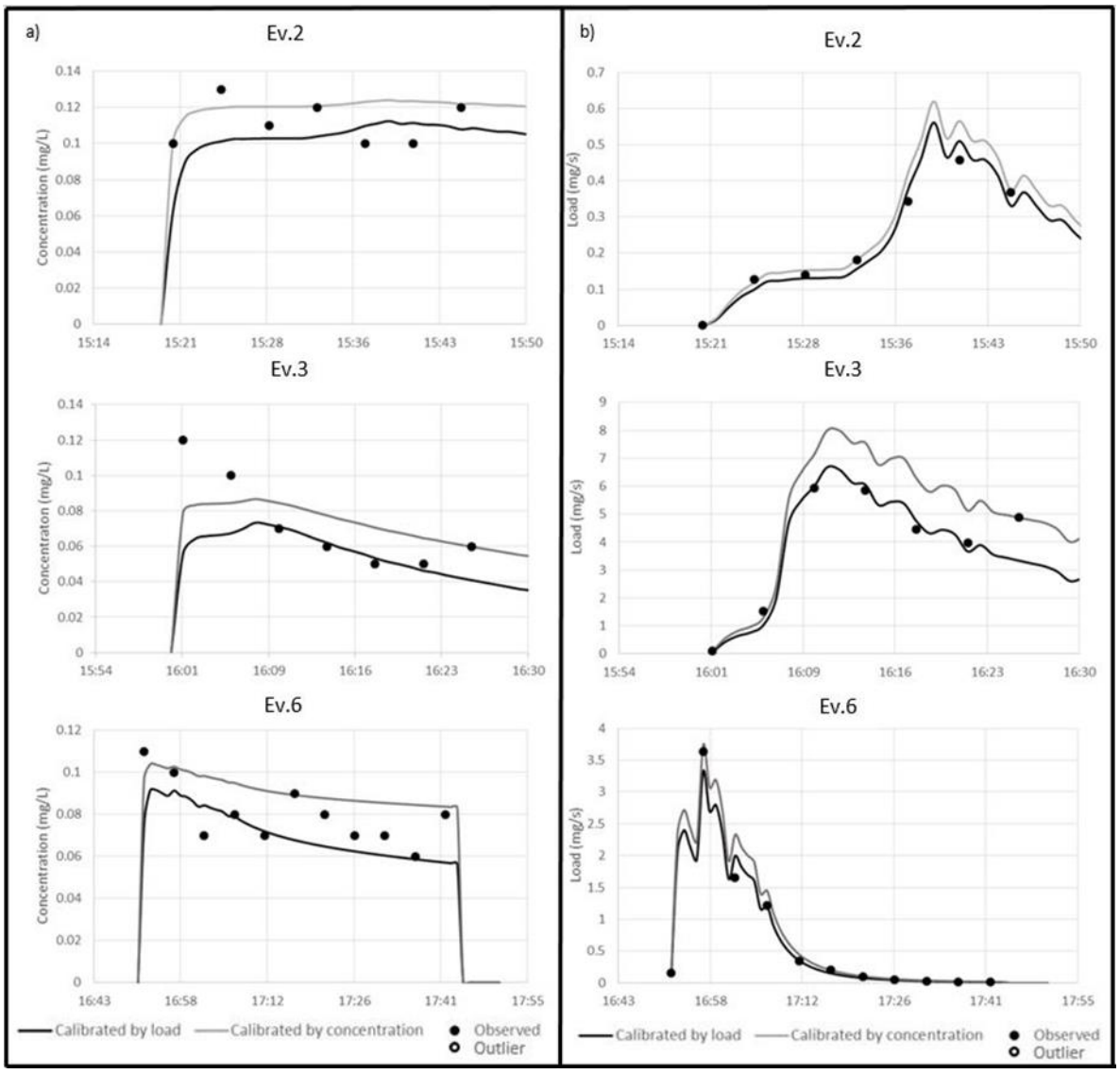

A11 – TOC calibration and validation

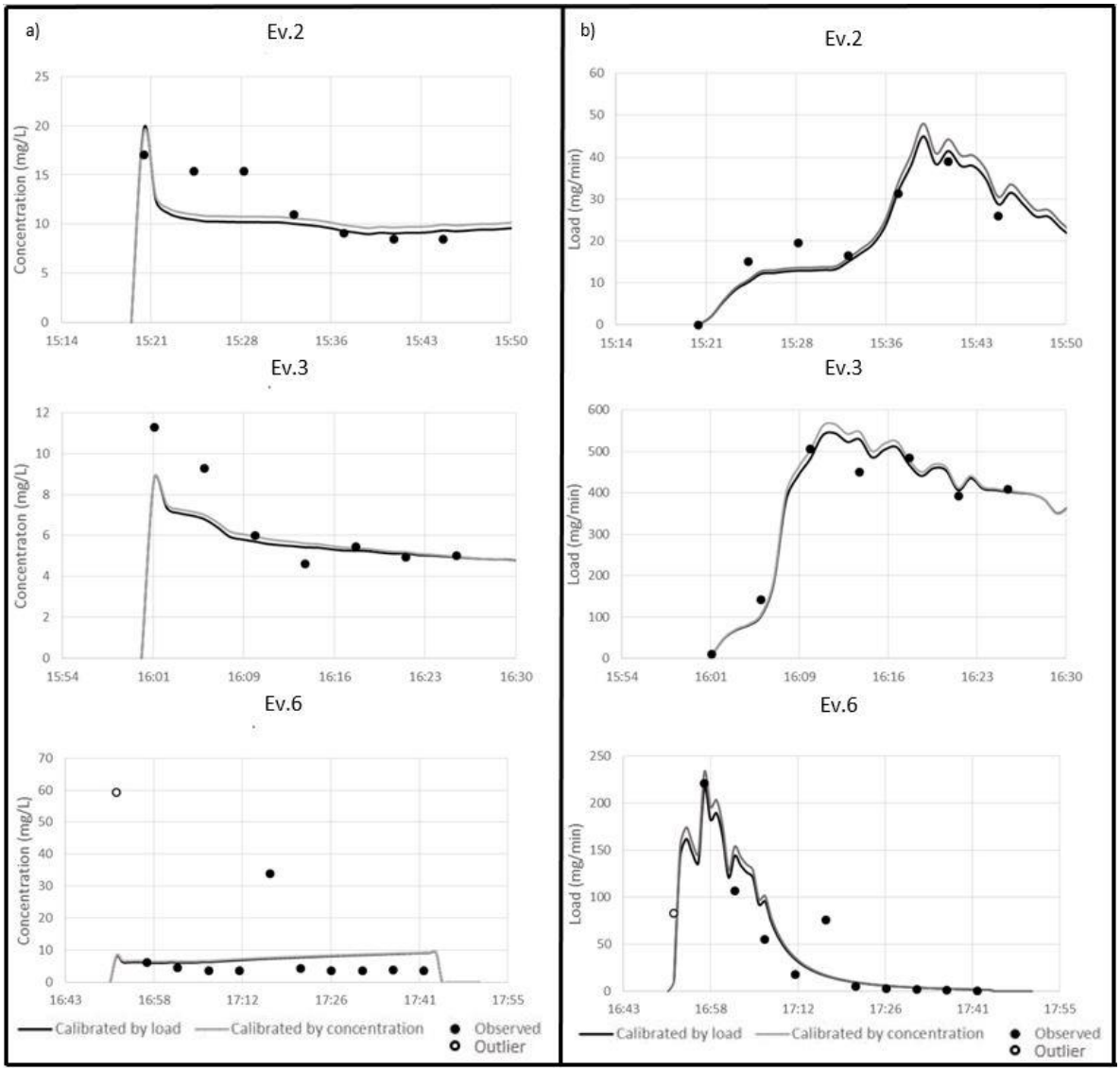

A12 – Zn calibration and validation

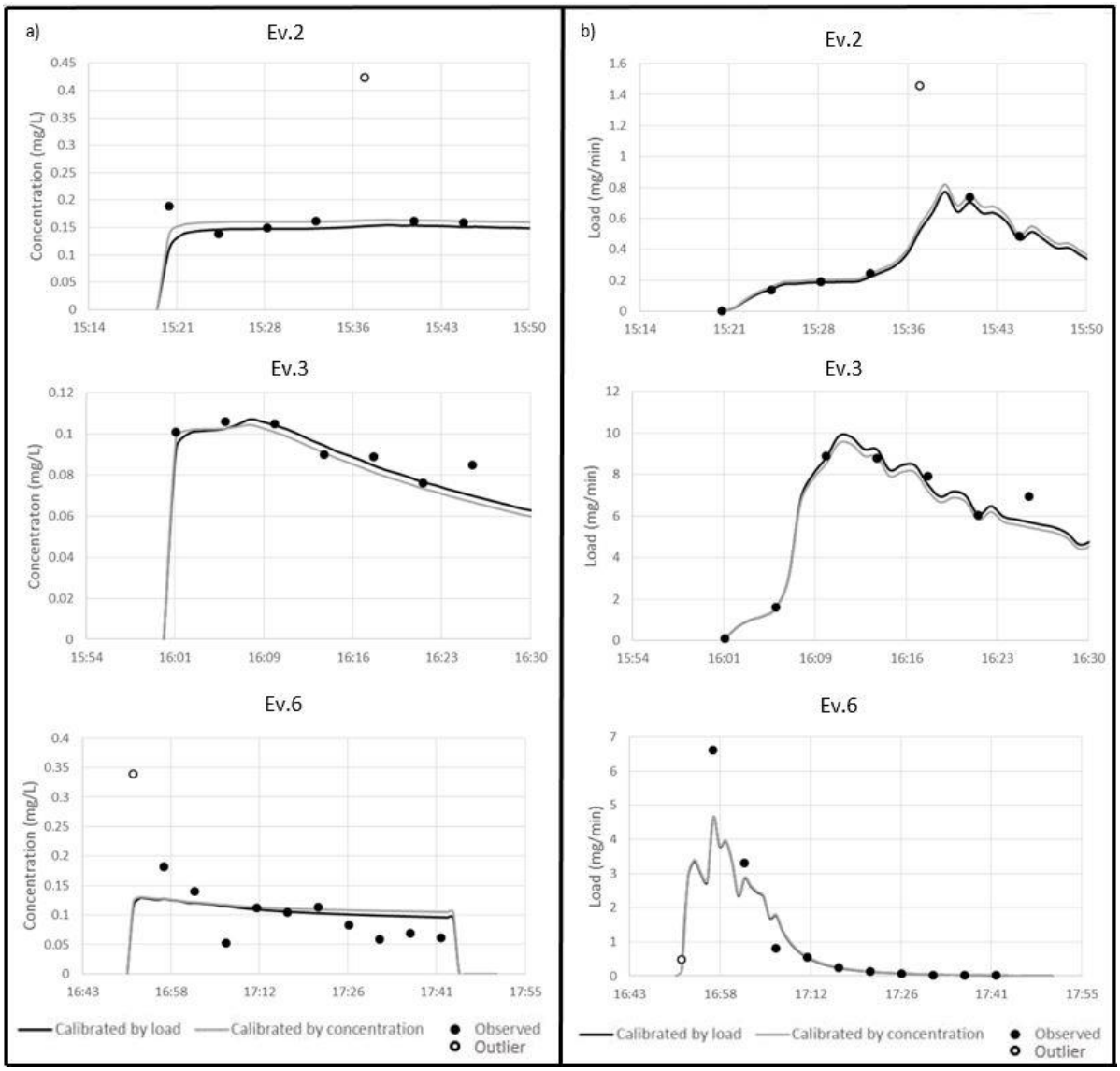

A13 – Bioretention outflow calibration (Ev4- Ev7)

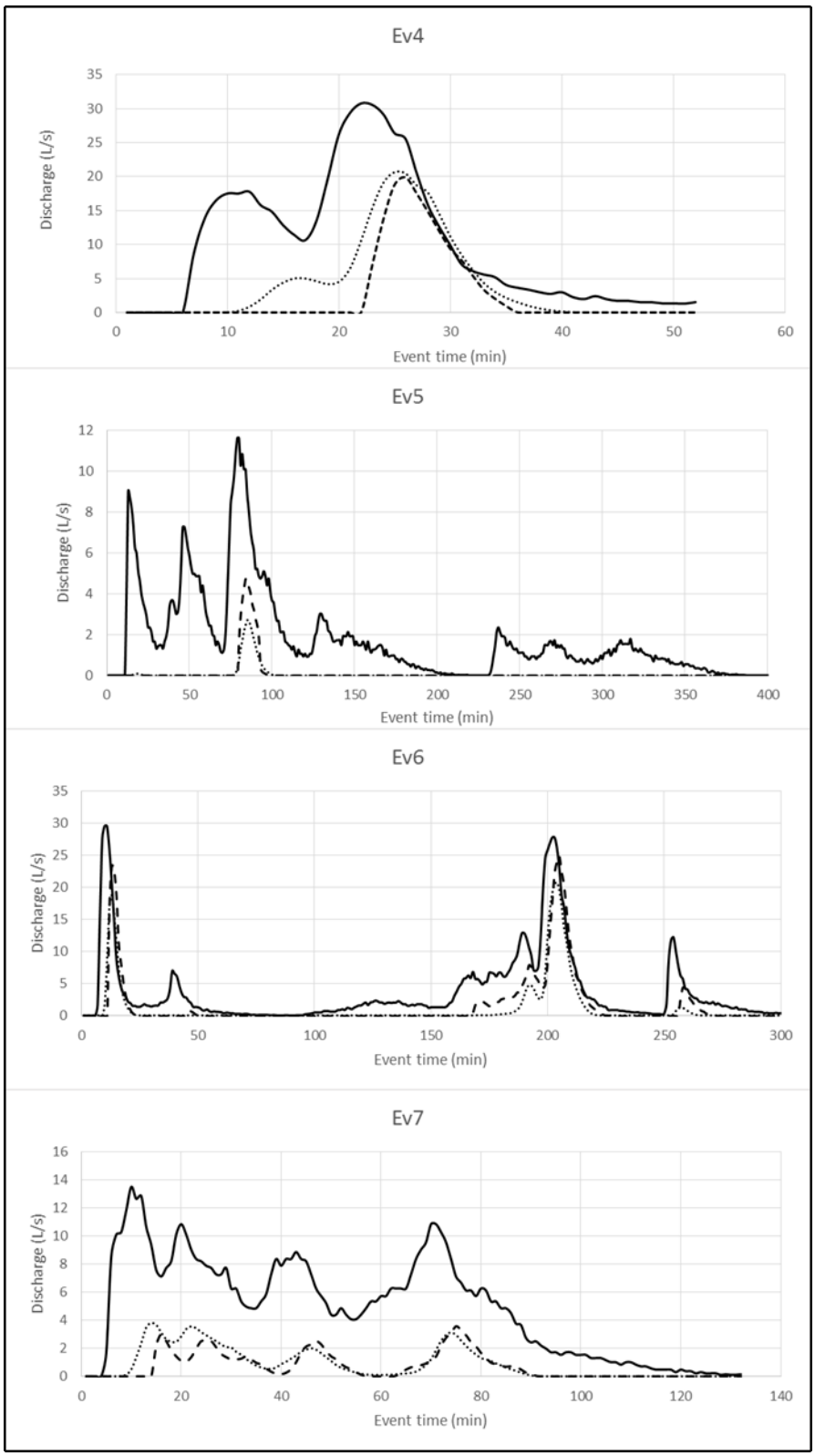

A14 – Bioretention outflow validation (Ev8, Ev10 and Ev11)

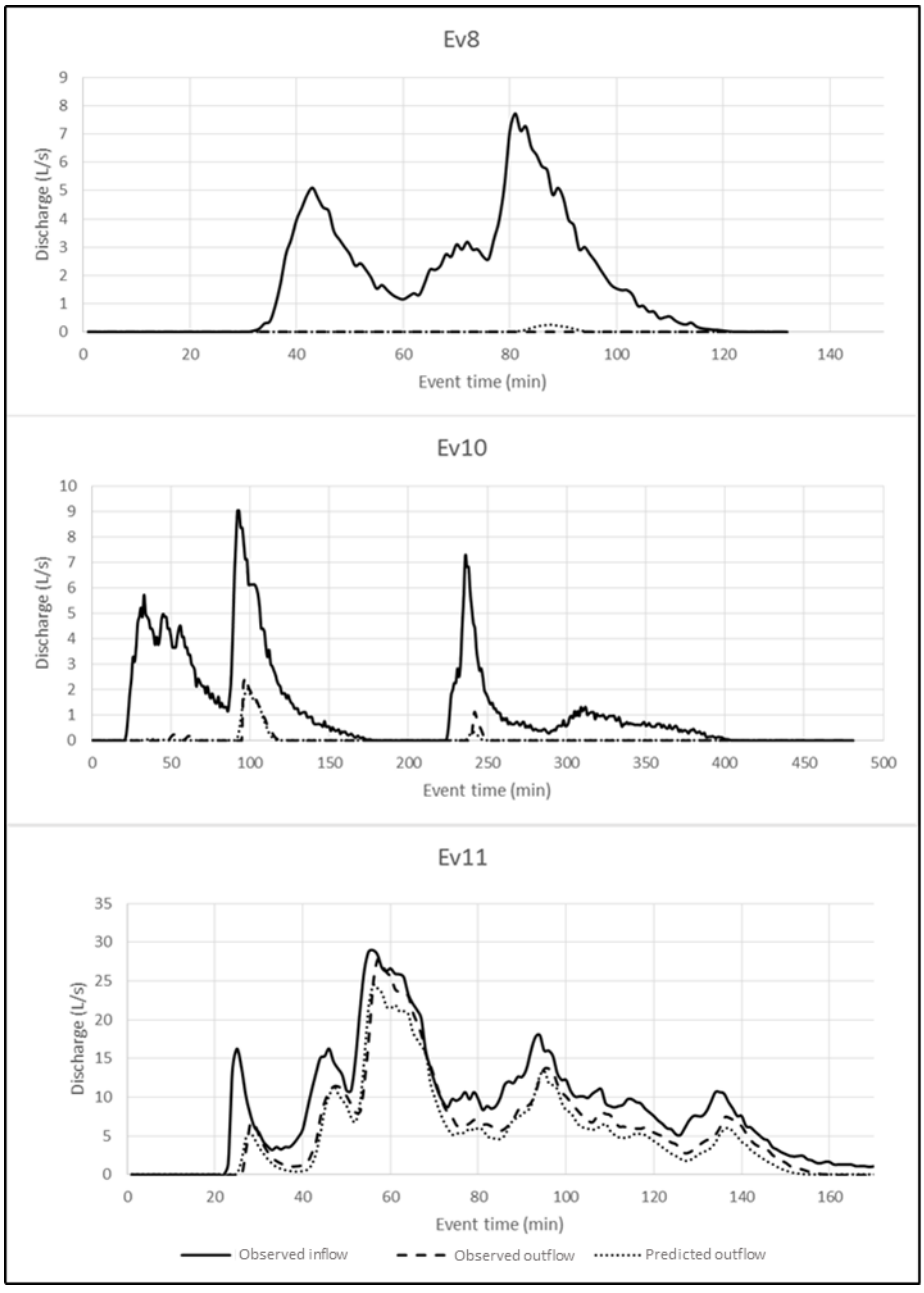

A15 – Desegregated and observed wet cells (Jan to Jun)

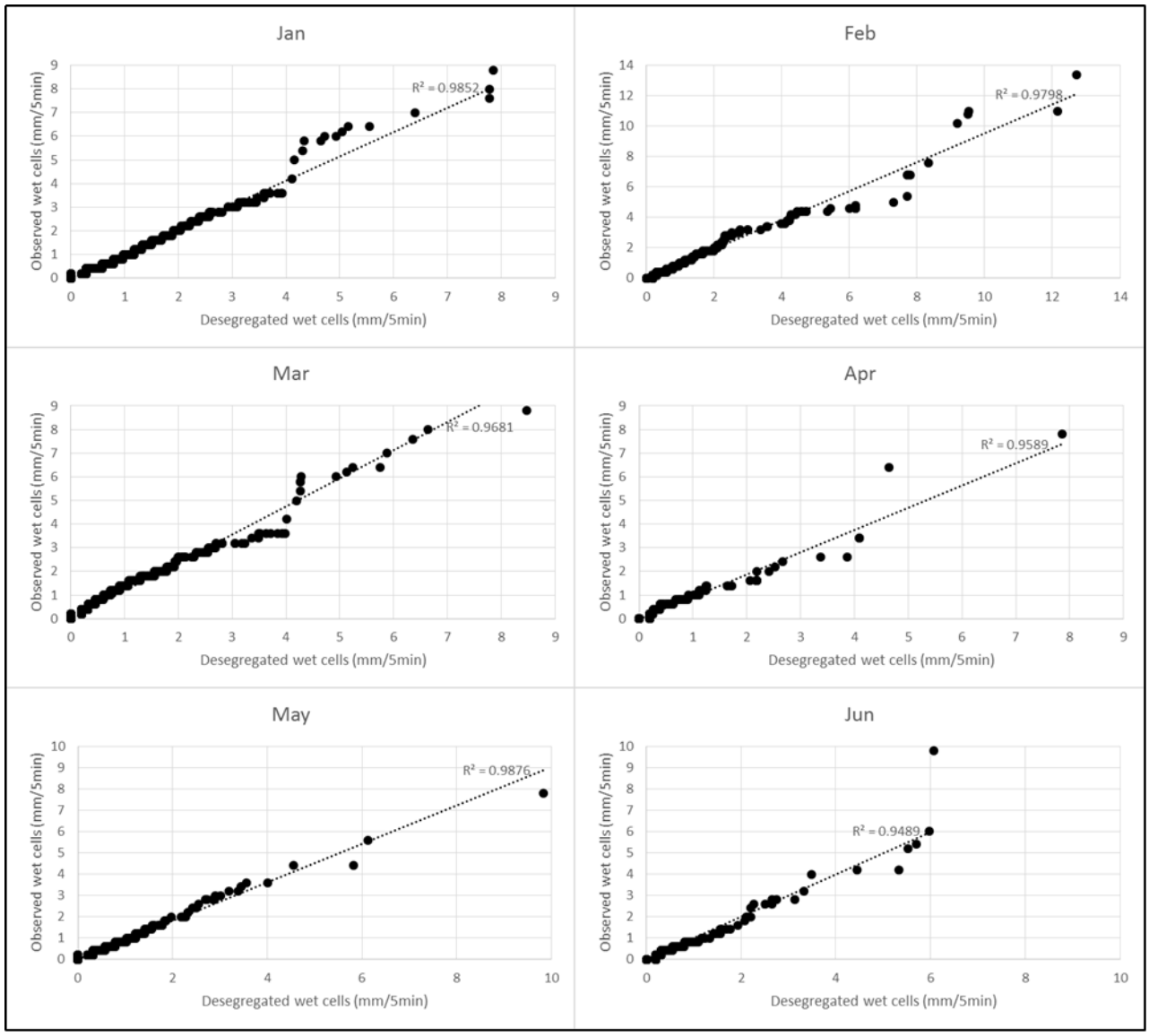

A16– Desegregated and observed wet cells (Jul to Dec)